HHS Public Access

Author manuscript

J Med Chem. Author manuscript; available in PMC 2024 September 14.

Published in final edited form as:

J Med Chem. 2023 September 14; 66(17): 12249–12265. doi:10.1021/acs.jmedchem.3c00806.

Structure–Activity Relationship of Truncated 2,8-Disubstituted-Adenosine Derivatives as Dual A_{2A}/A_3 Adenosine Receptor Antagonists and Their Cancer Immunotherapeutic Activity

Gibae Kim,
Research Institute of Pharmaceutical Sciences, College of Pharmacy, Seoul National University, Seoul 08826, Republic of Korea

Xiyan Hou,
Research Institute of Pharmaceutical Sciences, College of Pharmacy, Seoul National University, Seoul 08826, Republic of Korea; College of Life Science, Dalian Minzu University, Dalian 116600, People's Republic of China

Woong Sub Byun,
Research Institute of Pharmaceutical Sciences, College of Pharmacy, Seoul National University, Seoul 08826, Republic of Korea; Department of Chemical and Systems Biology, Chem-H and Stanford Cancer Institute, Stanford School of Medicine, Stanford University, Stanford, California 94305, United States

Gyudong Kim,
Research Institute of Pharmaceutical Sciences, College of Pharmacy, Seoul National University, Seoul 08826, Republic of Korea; College of Pharmacy & Research Institute of Drug Development, Chonnam National University, Gwangju 61186, Republic of Korea

Dnyandev B. Jarhad,
Research Institute of Pharmaceutical Sciences, College of Pharmacy, Seoul National University, Seoul 08826, Republic of Korea

Grim Lee,

Corresponding Author: **Lak Shin Jeong** – *Research Institute of Pharmaceutical Sciences, College of Pharmacy, Seoul National University, Seoul 08826, Republic of Korea; Future Medicine Company Limited, Seoul 06665, Republic of Korea*; lakjeong@snu.ac.kr.

Author Contributions

G.K., X.H., G.K., D.B.J., G.L., Y.E.H., J.Y., C.S.L., S.Q., and L.S.J. participated in the structural drug design. G.K., X.H., G.K, D.B.J., and G.L. synthesized the compounds. W.S.B. and S.K.L. performed an *in vivo* efficacy test. G.K., G.K., and D.B.J. determined the X-ray crystal structure. E.W., Z.-G.G., and K.A.J. performed *in vitro* binding affinity G.K. performed the molecular docking study. J.Y.K. and H.W.L. conducted an *in vivo* pharmacokinetic test and an *in vitro* ADME assay. E.W., Z.-G.G., S.J., H.S., J.-R.C., and K.A.J. performed an *in vitro* cAMP functional assay. H.W.L., K.A.J., S.K.L., and L.S.J. supervised the project. L.S.J. wrote the article with inputs from all co-authors. All authors have given approval to the final version of the manuscript.

Supporting Information

The Supporting Information is available free of charge at https://pubs.acs.org/doi/10.1021/acs.jmedchem.3c00806.

Additional *in vitro* data, X-ray crystallography data, HPLC data of representative final compounds, and ^{1}H and ^{13}C NMR copies of intermediates and all final compounds **5a–5v** (PDF)

Coordinate file for the docking model of compound **3a** to $A_{2A}AR$, coordinate file for the docking model of compound **5a** and **5j** to $A_{2A}AR$, and coordinate file for the homology docking model of compound **5a** and **5j** to A_3AR (ZIP)

Molecular formula strings (CSV)

Complete contact information is available at: https://pubs.acs.org/10.1021/acs.jmedchem.3c00806

The authors declare no competing financial interest.

Research Institute of Pharmaceutical Sciences, College of Pharmacy, Seoul National University, Seoul 08826, Republic of Korea

Young Eum Hyun,
Research Institute of Pharmaceutical Sciences, College of Pharmacy, Seoul National University, Seoul 08826, Republic of Korea

Jinha Yu,
Research Institute of Pharmaceutical Sciences, College of Pharmacy, Seoul National University, Seoul 08826, Republic of Korea; College of Pharmacy and Graduate School of Pharmaceutical Sciences, Ewha Womans University, Seoul 03760, South Korea

Chang Soo Lee,
Research Institute of Pharmaceutical Sciences, College of Pharmacy, Seoul National University, Seoul 08826, Republic of Korea

Shuhao Qu,
Research Institute of Pharmaceutical Sciences, College of Pharmacy, Seoul National University, Seoul 08826, Republic of Korea

Eugene Warnick,
Molecular Recognition Section, Laboratory of Bioorganic Chemistry, National Institute of Diabetes, and Digestive and Kidney Disease, National Institutes of Health, Bethesda, Maryland 20892, United States

Zhan-Guo Gao,
Molecular Recognition Section, Laboratory of Bioorganic Chemistry, National Institute of Diabetes, and Digestive and Kidney Disease, National Institutes of Health, Bethesda, Maryland 20892, United States

Ji Yong Kim,
Future Medicine Company Limited, Seoul 06665, Republic of Korea

Seunghee Ji,
HK Inno.N Corporation, Seoul 04551, Republic of Korea

Hyunwoo Shin,
HK Inno.N Corporation, Seoul 04551, Republic of Korea

Jong-Ryoul Choi,
HK Inno.N Corporation, Seoul 04551, Republic of Korea

Kenneth A. Jacobson,
Molecular Recognition Section, Laboratory of Bioorganic Chemistry, National Institute of Diabetes, and Digestive and Kidney Disease, National Institutes of Health, Bethesda, Maryland 20892, United States

Hyuk Woo Lee,
Future Medicine Company Limited, Seoul 06665, Republic of Korea

Sang Kook Lee,

Research Institute of Pharmaceutical Sciences, College of Pharmacy, Seoul National University, Seoul 08826, Republic of Korea

Lak Shin Jeong
Research Institute of Pharmaceutical Sciences, College of Pharmacy, Seoul National University, Seoul 08826, Republic of Korea; Future Medicine Company Limited, Seoul 06665, Republic of Korea

Abstract

Based on $hA_{2A}AR$ structures, a hydrophobic C8-heteroaromatic ring in 5′-truncated adenosine analogues occupies the subpocket tightly, converting $hA_{2A}AR$ agonists into antagonists while maintaining affinity toward hA_3AR. The final compounds of 2,8-disubstituted-N^6-substituted 4′-thionucleosides, or 4′-oxo, were synthesized from D-mannose and D-erythrono-1,4-lactone, respectively, using a Pd-catalyst-controlled regioselective cross-coupling reaction. All tested compounds completely antagonized $hA_{2A}AR$, including **5d** with the highest affinity ($K_{i,A_{2A}}$ = 7.7 ± 0.5 nM). The $hA_{2A}AR$–**5d** X-ray structure revealed that C8-heteroaromatic rings prevented receptor activation-associated conformational changes. However, the C8-substituted compounds still antagonized hA_3AR. Structural SAR features and docking studies supported different binding modes at $A_{2A}AR$ and A_3AR, elucidating pharmacophores for receptor activation and selectivity. Favorable pharmacokinetics were demonstrated, in which **5d** displayed high oral absorption, moderate half-life, and bioavailability. Also, **5d** significantly improved the antitumor effect of anti-PD-L1 *in vivo*. Overall, this study suggests that the novel dual $A_{2A}AR/A_3AR$ nucleoside antagonists would be promising drug candidates for immune-oncology.

Graphical Abstract

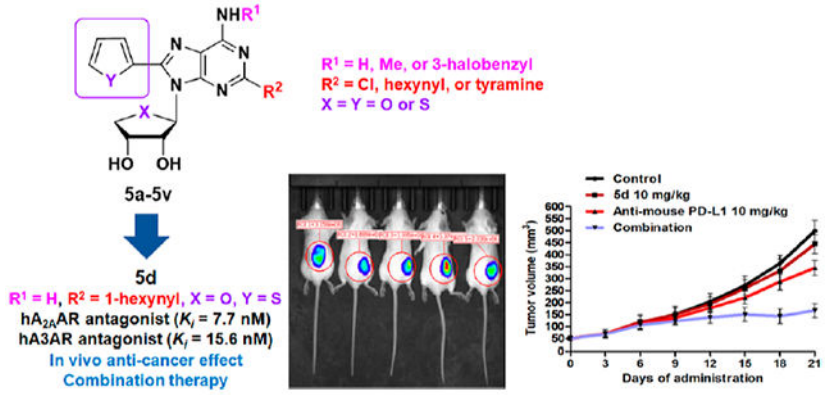

INTRODUCTION

Although there has been remarkable progress in anticancer therapy, cancer remains the main life-threatening disease.[1] Recently, immuno-oncology agents emerged as the next generation of antitumor drugs for immune checkpoint inhibition.[2] Among them, monoclonal antibodies (mAbs) have been intensively studied as immune checkpoint inhibitors.[3] They block costimulatory molecules on immune cells and inhibit immune-evasion of a tumor, resulting in the reactivation of the immune system. However, mAb immune checkpoint

inhibitors have some limitations such as their high cost, prolonged half-life, immune-related adverse effects, and immunogenicity.[4] To overcome these drawbacks, the development of small molecules as immuno-oncology agents has been highly appealing. A number of target proteins such as toll-like receptors (TLRs), stimulators of interferon genes (STING), adenosine receptors (ARs), and so on have been investigated as the principal targets for the development of small molecule immune-oncology agents.[5]

ARs consist of four subtypes termed A_1, A_{2A}, A_{2B}, and A_3. Among these, A_{2A}AR and A_{2B}AR couple to G_S protein, which activates adenylate cyclase (AC) to increase the level of cyclic AMP (cAMP), while A_1AR and A_3AR bind to G_i protein, inhibiting the level of cAMP. In a tumor microenvironment (TME), ecto-5′-nucleotidase (CD73) on the cell surface catalyzes the hydrolysis of extracellular adenosine-5′-monophosphate (AMP) to adenosine and phosphate, resulting in high adenosine concentrations. When adenosine is released in the tumor microenvironment, it can activate any of the four AR subtypes to control cAMP levels.[6] Notably, adenosine activating the A_{2A}AR, which is overexpressed in effector T cells and then blocks T cell receptor (TCR) signaling, abolishes the immune response.[7] In addition, A_{2A}AR also upregulates the expression of negative costimulatory molecules such as programmed cell death 1 (PD-1) and cytotoxic T-lymphocyte antigen 4 (CTLA4), stimulating immune evasion.[8] Thus, if A_{2A}AR is blocked, immune checkpoints by CTLA4, PD-1, or PD-L1 can be inhibited in cancer cells, giving A_{2A}AR antagonists cancer immunotherapeutic potential. Furthermore, an A_{2A}AR antagonist is expected to show a synergistic effect in combination with mAb immune checkpoint inhibitors.[9] In fact, most of the A_{2A}AR antagonists in clinical trials as cancer immunotherapeutic agents, are coadministered with a mAb immune checkpoint inhibitor as combination therapy.[10]

Based on a potent and selective A_3AR agonist, 2-chloro-N^6-(3-iodobenzyl)adenosine-5′-*N*-methyluronamide (Cl-IB-MECA, **1a**),[13] we have long been interested in discovering new AR ligands with the 4′-thionucleoside skeleton. Among these, 2-chloro-N^6-(3-iodobenzyl)-4′-thioadenosine-5′-*N*-methyluronamide (thio-Cl-IB-MECA, **1b**)[14] was discovered to be a more potent human (h) A_3AR agonist (K_i = 0.38 ± 0.07 nM) than **1a** (K_i = 1.4 ± 0.3 nM) (Chart 1). Truncation of the 5′-uronamide of **1a** and **1b** converted selective A_3AR agonists **1a** and **1b** into A_3AR antagonists **2a** (K_i = 42.9 ± 8.9 nM) and **2b** (K_i = 4.16 ± 0.5 nM).[15] From this study, the amide proton of the 5′-uronamide group of **1a** and **1b** acted as a hydrogen-bonding donor, which was essential for the induced fit in the receptor required for A_3AR agonism. Compound **2b** also showed high binding affinity (K_i = 3.89 ± 1.15 nM) at the rat A_3AR, indicating that it is a species-independent A_3AR antagonist. These truncated nucleosides **2a** and **2b** were the first examples to show pure A_3AR antagonism with species-independent and high binding affinity with a nucleoside skeleton,[15] potentially for treatment of chronic kidney disease (CKD)[16] and cancer.[17] Further SAR study of **2a** and **2b** at the C2 and N^6-positions resulted in the discovery of A_{2A}AR agonists **3a** (K_i = 63.2 ± 15 nM) and **3b** (K_i = 7.19 ± 0.6 nM), in which an extended hexynyl group at the C2 position and a free amino group at the N^6-position were found to act as essential pharmacophores for A_{2A}AR binding, although they also maintained the antagonistic activity at the hA_3AR.[18]

In order to switch compound **3** to an A_{2A}AR antagonist, we analyzed agonist- and antagonist-bound co-crystal structures of the A_{2A}AR. As shown in Figure 1, A_{2A}AR antagonist (ZM-241385) occupied a subpocket which was expanded by $His250^{6.52/A2A}$ (Figure 1A, $His250^{6.52/A2A}$; Ballesteros–Weinstein residue numbering and name of the receptor are referred to as superscripts.[19]). Also, the predicted binding mode of **3a** with hA_{2A}AR indicated that the C8 position is located in a spacious subpocket capable of accommodating a bulky substituent (Figure 1B, yellow). Thus, if we introduce an aromatic ring at the C8 position of **3a**, it was hypothesized that it induces tight binding rather than an induced fit required for receptor activation, anticipating the conversion of A_{2A}AR agonist **3b** into A_{2A}AR antagonist **4.** As expected, compound **4** was found to be a full A_{2A}AR antagonist (K_i = 18.3 ± 4.8 nM). Recently, we reported the X-ray co-crystal structure complexed with A_{2A}AR antagonist **4**,[11] confirming our hypothesis that the C8 aromatic ring of **3a** tightly binds to the subpocket and serves as the key pharmacophoric feature to discriminate between agonist and antagonist.[18,20] Most known A_{2A}AR agonists possess a nucleoside structure, while all known A_{2A}AR antagonists have heterocyclic compounds without a sugar ring.[10] These results indicate that both 2′–OH and 3′–OH groups have a pivotal role for A_{2A}AR activation but are not essential for an inactive A_{2A}AR state.[20] Namely, despite possessing a nucleoside skeleton containing both 2′–OH and 3′–OH, the compounds of this research exhibited potent A_{2A}AR antagonism, and it is believed to be the first example.[11]

Based on these findings, we carried out a comprehensive SAR study at the C2-, C8-, and N^6-positions of **4**, synthesized the truncated 4′-oxonucleoside derivatives **5a–f** and measured their A_{2A}AR binding affinities.[20] Also, we synthesized the corresponding truncated 4′-thionucleosides **5g–v**, based on a bioisosteric relationship between oxygen and sulfur, and evaluated them for binding affinities of the four adenosine receptor subtypes.[12]

Herein, we report the design, synthesis, and binding affinity of the final nucleosides **5**, modified at the C2, C8, and N^6-positions. We also report the pharmacokinetic characterization and *in vivo* antitumor effects of the most potent A_{2A}AR antagonist in the series for its development as an immuno-oncology agent.

RESULTS AND DISCUSSION

Chemistry.

The 4′-oxonucleoside derivatives **5a–f** were synthesized from D-erythrono-1,4-lactone, as shown in Scheme 1. D-Erythrono-1,4-lactone was protected as 2,3-*O*-acetonide under the standard conditions, which was reduced with diisobutylaluminum hydride (DIBAL-H) to afford lactol **6**.[15] Acetylation of lactol **6** afforded the glycosyl donor **7**.[15c] Condensation of **7** with silylated 6-chloropurine under Vorbrüggen[21] conditions in the presence of trimethylsilyl trifluoromethansulfonate (TMSOTf) as a Lewis acid yielded the protected *β*-nucleoside **8** as a single stereoisomer. Treatment of **8** with 1 N HCl followed by the protection of resulting diol with the *t*-butyldimethylsilyl (TBS) group afforded the di-*O*-TBS ether, which was subjected to the iodination[22] at C2 and C8 positions using a freshly prepared lithium tetramethylpiperidide (LiTMP) to produce 6-chloro-2,8-

diiodo-purine derivative **9**. Palladium catalyst-controlled regioselective Sonogashira[22–24] coupling of **9** with 1-hexyne in the presence of tetrakis(triphenylphosphine)palladium and cesium carbonate yielded C2-hexynyl derivative **10** as the major regioisomer.[23] Then, another palladium-catalyzed Stille[25] coupling of **10** with 2-tributylstannylfuran and–thiophene yielded the C8-furyl derivative **11a** and the C8-thienyl derivative **11b**, respectively, after desilylation. The regio- and stereochemistry of **11b** were confirmed by X-ray crystallography (Scheme 1, please see the Supporting Information for the X-ray crystallographic details of the compound **11b**). Compounds **11a** and **11b** were treated with ammonia, methylamine, and 3-iodobenzylamine to afford **5a–c** and **5d–f**, respectively.

Next, we synthesized the corresponding 4′-thionucleoside derivatives **5g–v**, based on the bioisosteric relationship between oxygen and sulfur. The synthetic strategy to the 4′-thionucleoside derivatives **5g–v** was to condense the glycosyl donor **16** with 6-chloro-2,8-diiodopurine **17d** or 2,6-dichloro-8-iodopurine **19** under Vorbrüggen[21] conditions and then apply regioselective C8-Stille[25] coupling, C2-Sonogashira[22–24] coupling, and N^6-amination on the purine moiety. Thus, we first synthesized the glycosyl donor **16** from D-mannose according to our previously published procedure (Scheme 2).[26]

D-Mannose was treated with 2,2-dimethoxypropane in the presence of camphorsulfonic acid to give di-*O*-acetonide, which was reduced with $NaBH_4$, and the resulting diol was treated with mesyl chloride to give the dimesylate **12** in 82% yield. Treatment of **12** with Na_2S in DMF at 80 °C afforded the 4-thiosugar, which was selectively hydrolyzed with 60% acetic acid to give 5,6-diol **13**. As the 2,3-acetonide was problematic for removal under acidic conditions at the final step, the 2,3-*O*-acetonide was converted to the 2,3-di-*O*-TBS group as follows. Benzoylation of **13**, followed by hydrolysis of 2,3-*O*-acetonide with 80% acetic acid, yielded 2,3-diol **14**. Protection of diol **14** with a TBS group followed by the removal of the benzoyl group afforded 5,6-diol **15**. Oxidative cleavage of **15** with $Pb(OAc)_4$ yielded the glycosyl donor **16**.

Then, we synthesized 6-chloro-2,8-diiodopurine **17d** and 2,6-dichloro-8-iodopurine **19**, which can serve as essential intermediates for selective modification at the C2, C8, and N^6 positions (Scheme 3). N^6-Protected 6-chloropurine (**17a**)[27] was treated with LiTMP, prepared by treating tetramethylpiperidine with *n*-BuLi, followed by treatment with iodine to yield 2,8-diiodo derivative **17c**.[22] Because the 8-iodo position was sensitive to degradation under acidic conditions, the tetrahydropyran (THP) group of **17c** was removed with $CuCl_2$ to afford **17d**. N^9-Protected 2,6-dichloropurine **17b**[27] was treated with lithium diisopropylamide (LDA), prepared by treating *i*-Pr_2NH with *n*-BuLi, followed by further treatment with iodine to give 8-iodo derivative **18**. The removal of the THP group of **18** under mild acidic conditions afforded **19**.

Condensation of **16** with silylated 6-chloro-2,8-diiodopurine in the presence of TMSOTf[21] as a Lewis acid yielded the protected nucleoside **20** as a single β-anomer without concomitant formation of the N^7-isomer. The desired C2-selectivity was not observed in substrate **20** when we attempted regioselective Sonogashira coupling, as shown in Scheme 1. Thus, we paid attention to Stille coupling to obtain the desired product. Delightfully, we were able to regioselectively synthesize 8-furyl derivative **21a** and the 8-thienyl derivative

21b regioselectively with high yield. The 2-hexynyl derivatives **22a** and **22b** were then synthesized *via* another palladium-catalyzed Sonogashira coupling of **21a** and **21b** with 1-hexyne, respectively, and their structures were confirmed by X-ray crystallography (Scheme 4, please see Supporting Information for the X-ray crystallographic details of the compounds **22a** and **22b**). N^6-Substitution of **22a** and **22b** with ammonia, methylamine, and 3-iodobenzylamine afforded the final nucleosides **5g–i** and **5j–l**, respectively.

Then, we synthesized the N^6,C8-disubstituted-4′-thioadenosines **5m–v** with chloro or *p*-hydroxyphenethylamine (tyramine) groups at the C2 position because a selective A_{2A} antagonist, 4-(2-[7-amino-2-(2-furyl)[1,2,4]triazolo[2,3-*a*]-[1,3,5]triazin-5-ylamino]ethyl) phenol (ZM-241385) possessed a C2-tyramine group[29] (Scheme 5). The glycosyl donor **16** was condensed with silylated 2,6-dichloro-8-iodopurine under Vorbrüggen[21] conditions to afford the condensed nucleoside **23**. Compound **23** was subjected to palladium-catalyzed Stille[25] coupling with 2-tributylstannylfuran and -thiophene to give 8-furyl- and 8-thienyl derivatives **24a** and **24b**, respectively. Treatment of **24a** and **24b** with tetra-*n*-butylammonium fluoride (TBAF), followed by further treatment of resulting diol derivatives with ammonia, methylamine, and 3-iodobenzylamine afforded the N^6-amino-, methylamino-, and 3-iodobenzylamino derivatives **5m–o** and **5p–r**, respectively. Furthermore, 2-chloro-8-furyl-N^6-amino- and methylamino derivatives **5m** and **5n** were converted to the corresponding 2-*p*-hydroxyphenethylamino derivatives **5s** and **5t**, respectively. Similarly, 8-thienyl derivatives **5p** and **5q** were converted to **5u** and **5v**, respectively.

Structure–Activity Relationship Studies and Pharmacological Profiles.

Binding Affinities and cAMP Functional Data to Adenosine Receptor Subtypes.—

The binding affinities of all final nucleosides **5a–v** at the four subtypes of the hARs were measured using standard radioligands and membrane preparations.[29] The hA_1AR and hA_3AR were expressed in Chinese hamster ovary (CHO) cells, and the $hA_{2A}AR$ and $hA_{2B}AR$ were expressed in human embryonic kidney (HEK)-293 cells. [$_3$H](−)-N^6-2-Phenylisopropyladenosine (**25**, R-PIA), [$_3$H]2-[*p*-(2-carboxyethyl)phenylethylamino]-5′-*N*-ethylcarboxamido-adenosine (**26**, CGS21680), 1,3-[$_3$H]-dipropyl-8-cyclopentylxanthine (**27**, DPCPX), and [^{125}I]N^6-(4-amino-3-iodobenzyl)-5′-*N*-methylcarboxamidoadenosine (**28**, I-AB-MECA) were used for the hA_1AR, $hA_{2A}AR$, $hA_{2B}AR$, and hA_3AR, respectively. The percent inhibition of radioligand binding at 10 μM was reported in cases of weak binding. Nonspecific binding was defined using 5′-*N*-ethylcarboxamidoadenosine (**29**, NECA).

As shown in Table 1, the addition of a hydrophobic furan or thiophene ring at the C8 position of **3** preserved considerable AR affinity in general and at the $A_{2A}AR$, specifically. The furan substitution exhibited comparable $hA_{2A}AR$ binding affinity with the thiophene substitution, although the orientation of thiophene can be stabilized as a preferred binding pose by the 1,4-N…S noncovalent sulfur interaction between thiophene and N^7 nitrogen.[30] It implies that the interaction between $hA_{2A}AR$ and the heteroatom of the C8-aromatic ring is not crucial for binding with the receptor. As the C2 position is appended with a rigid and hydrophobic hexyne substituent (**5a–5l**), the addition of a hydrophobic group at the N^6-position decreased $hA_{2A}AR$ binding affinity in the following order: R^1 = H

> CH_3 > 3-iodobenzyl. This pattern indicated that a free amino group is essential for appropriate hydrogen bonding in the $hA_{2A}AR$, which matches our previous findings.[18] In the case of the binding affinities of C2-hexyne compounds for hA_3AR, the 4′-thionucleoside derivatives (**5g–5l**) could not tolerate the bulky N^6-3-iodobenzylamine, as opposed to the 4′-oxonucleoside derivatives (**5a–5f**) and the series of compounds with C8–H substitution.[18b] On the other hand, 2-Cl or 2-tyramine compounds (**5m–5v**) favored bulkier N^6-substituents than free amines. These results indicate that the tight binding by both bulky C8-aromatic ring and rigid C2-hexyne can contract the binding pocket near N^6-position. In the N^6-NH_2 derivatives, the C2-hexyne compounds maintained substantial binding affinity at the hA_{2A} and hA_3ARs, but 2-Cl or 2-tyramine substitution decreased the binding affinities at both receptors dramatically. It is surprising in that a C2-tyramine substitution[28] was reported to increase the binding affinity at the $hA_{2A}AR$. In general, 4′-oxonucleoside derivatives exhibited better binding affinities at the $hA_{2A}AR$ and hA_3AR than the corresponding 4′-thionucleoside derivatives, among which **5d** exhibited the best binding affinity at the $hA_{2A}AR$ (K_i = 7.7 ± 0.5 nM) along with good binding affinity at the hA_3AR (K_i = 15.6 ± 1.6 nM). Among tested 4′-thionucleoside derivatives, compound **5g** exhibited the highest binding affinity (K_i = 13.2 ± 0.2 nM at $hA_{2A}AR$) with high selectivity ($K_{i,5g}$ = 119 ± 39 nM at hA_3AR). These findings provide an essential clue leading to the discovery of selective nucleoside $A_{2A}AR$ ligands.

Three synthesized compounds were evaluated in functional cAMP assays in $hA_{2A}AR$- or hA_3AR-expressing CHO cell lines. As shown in Table 2, no receptor activation at the $hA_{2A}AR$ at 10 μM concentration for compounds **5a**, **5d**, and **5g** was observed, demonstrating that they act as $hA_{2A}AR$ full antagonists. Among them, the compound **5d** demonstrated the highest potency, and its K_B value was calculated to be 25.8 nM at the $hA_{2A}AR$ using full agonist NECA (**29**) (Table S1). Similarly, compounds **5a**, **5d**, and **5g** inhibited hA_3AR activation at 10 μM, and the K_B value of **5d** for hA_3AR was calculated to be 107.4 nM, also indicating that it is a full hA_3AR antagonist. It should be noted that the addition of a hydrophobic furan or thiophene at the C8 position could convert $A_{2A}AR$ agonists into $A_{2A}AR$ antagonists successfully by inhibiting the interaction for receptor inactivation.

Molecular Docking Studies.—In order to elucidate the effect of 4′-thioribose, a homology modeling study was performed using the co-crystal structure of $A_{2A}AR$ containing **5d** (Figure 2, PDB ID: 8CU6). Comparison of the binding sites of $hA_{2A}AR$ and hA_3AR revealed two characteristic differences that can induce variation in binding affinity between the two receptors: the expanded binding pocket by $Ser247^{6.52/A3}$ (blue arrow), and the reduced ribose-binding pocket by $Leu90^{3.32/A3}$ of hA_3AR (red arrow) (Figure 2A). Molecular docking was then performed for 4′-thionucleoside **5j** and 4′-oxonucleoside **5d**. Docking with the homology model of hA_3AR showed that the binding pose of **5d** was similar to that of $hA_{2A}AR$, whereas **5j** exhibited a reverse-oriented binding pose due to steric clashes between 4′-thioribose and $Leu90^{3.32/A3}$ (Figure 2B). In $hA_{2A}AR$, although there were minor steric clashes between $Ile274^{7.39/A2A}$/$His278^{7.43/A2A}$ and **5j**, the ligand could still retain its forward-oriented binding pose due to the smaller residue $Val84^{3.32/A2A}$ compared to $Leu90^{3.32/A3}$ (red dashed line, Figure 2C,D).

Overall, the molecular docking analysis suggests that steric clashes between the sugar moiety and the receptors can be a key factor in the binding of both $hA_{2A}AR$ and hA_3AR. Although the difference in the bulkiness of ribose can be considered subtle, as observed in the X-ray crystal structure of **11b** [C(4′)–O: 1.39 Å in ribose] and **22b** [C(4′)–S: 1.82 Å in 4′-thioribose], the results showed it was significant enough to result in several-fold changes in binding affinities and even flip the binding mode in hA_3AR (Figure 2B).

ADME Evaluation of Compound 5d.—We examined the druggability of the most potent compound **5d** primarily through *in vitro* ADME assays to determine its potential as a preclinical candidate. Our results showed that compound **5d** did not significantly inhibit five types of CYP isoforms (CYP1A2, CYP2C9, CYP2C19, CYP2D6, CYP3A4) and hERG K+ channels (Tables S2 and S3).

We also conducted an *in vivo* pharmacokinetic study of **5d** in mice, which revealed proper distribution (V_{ss} = 0.69 L/kg) and moderate plasma clearance (CL = 60.5 mL/min/kg). After oral administration, compound **5d** was rapidly absorbed (T_{max} = 0.25 h) with moderate bioavailability (F = 22.81%) and half-life ($t_{1/2}$ = 1.99 h) (Table 3).

Synergistic Antitumor Activity of Compound 5d with the Immune Checkpoint Inhibitor in 4T1-Luc Cells Implanted in Mouse Xenograft Models.—We conducted an *in vivo* test to investigate the antitumor effect of compound **5d** and its potential synergistic effect with an immune checkpoint inhibitor. 4T1-Luc tumor-bearing mice were intraperitoneally treated with compound **5d** (10 mg/kg), antimouse PD-L1 (10 mg/kg), or a combination of both treatments thrice per week for 21 days. As shown in Figure 3A–D, the single administration of compound **5d** resulted in a weak antitumor effect, with a TGI of 15%. However, coadministration of **5d** with antimouse PD-L1 demonstrated a substantial increase in TGI up to 77%, while the single administration of antimouse PD-L1 exhibited only 43% of TGI. No adverse effects or body weight loss were observed. In addition, bioluminescence imaging of mice was conducted on the final day of the experiment to precisely quantify the tumor mass. Consistent with the tumor volume decrease, the group of mice treated with combination therapy exhibited a remarkable reduction in signal intensity from the tumor (Figure 3E). Taken together, these results demonstrate that compound **5d** effectively improves the antitumor potential of the immune checkpoint inhibitor anti-PD-L1.

CONCLUSIONS

A series of truncated 4'-thio- and 4'-oxonucleoside derivatives substituted at C2, C8, and N_6-positions were synthesized from D-mannose and D-erythrono-1,4-lactone, respectively. Functional groups such as C2-hexynyl and C8-aryl groups were introduced by palladium catalyst-controlled regioselective cross-coupling.[22] From this study, it was discovered that the introduction of hydrophobic rings such as furan and thiophene at the C8 position successfully converted an $A_{2A}AR$ agonist into an $A_{2A}AR$ antagonist. The X-ray co-crystal structure of $hA_{2A}AR$ complexed with antagonist **5d**,[11] revealed that the subpocket was occupied by heteroaromatic rings, inducing tight binding that can abolish receptor activation. Additionally, the C8 substituent caused the ribose ring to rotate from its canonical orientation, disrupting a crucial interaction for receptor activation. Also, it was elucidated

that the C2-hexynyl group formed favorable hydrophobic interactions in a relatively large hydrophobic pocket of the A_{2A}AR.

4'-Oxonucleoside derivatives, **5a–5f**, showed better binding affinities than 4'-thionucleosides. Among them, compound **5d** was discovered as the best hA_{2A}AR antagonist (K_i = 7.7 ± 0.5 nM) along with a high antagonistic binding affinity at the hA_3AR (K_i = 15.6 ± 1.6 nM). Among the 4'-thionucleoside derivatives, **5g–5v**, the 4'-thionucleoside **5g** exhibited the highest binding affinity at hA_{2A}AR (K_i = 13.2 ± 0.2 nM), along with a ninefold stronger binding affinity than hA_3AR (K_i = 119 ± 39 nM). According to the molecular docking study, the steric clashes between 4′-thioribose and Leu90$^{3.32/A3}$ weaken the binding with A_3AR, flipping the binding pose of the ligand.

The most potent compound **5d** also showed good druggability and an acceptable pharmacokinetic profile suitable for a preclinical candidate. Furthermore, **5d** exhibited a potent *in vivo* antitumor effect as a combination therapy with the immune checkpoint inhibitor, anti-PD-L1, without any adverse effects and body weight loss.

A_{2A}AR antagonists are known to be highly associated with cancer immunotherapy activity. On the other hand, existing research demonstrates that the modulation of A_3AR can exhibit anticancer effects through distinct mechanisms, such as the induction of cell cycle arrest and inhibition of HIF-1α expression.[17,31] Hence, further investigation into the anticancer effects of compound **5d** will be conducted to elucidate its potential additive effect achieved through the modulation of A_3AR.

To the best of our knowledge, this is the first SAR study of A_{2A}AR antagonists with a nucleoside skeleton. The characteristics of the nucleoside moiety can provide beneficial effects such as species independence and pharmacokinetic properties, which are favorable for preclinical and clinical trials, as in the case of the A_3AR antagonist with a nucleoside skeleton.[15a,b] Thus, the novel nucleoside dual A_{2A}AR/A_3AR antagonist **5d** can be a promising drug candidate for combination therapy with immune checkpoint inhibitors.

EXPERIMENTAL SECTION

General Procedures.

The study employed various scientific techniques to measure and analyze the physical and chemical properties of synthesized compounds. NMR spectra (^{1}H/^{13}C) were obtained by Jeol JNM-ECZ 400s (400 MHz/100 MHz), Bruker AV500 (500 MHz/125 MHz), or Bruker AV800 (800 MHz/200 MHz) and reported as chemical shifts in parts per million (δ) relative to solvent peaks, with coupling constants (J) expressed in hertz (Hz). Melting points were measured using a Barnstead Electrothermal instrument, while optical rotations were obtained using a Jasco-P2000 instrument. Elemental analyses (C, H, and N) were conducted to assess compound purity, and HPLC (Agilent 1260 infinity series) was also used to determine the purities of the representative compounds using a binary solvent system [0.01 M KH_2PO_4 buffer in H_2O/MeCN] and an Agilent Zorbax Eclipse XDB-C18 column [5.0 μm, 4.6 mm i.d. × 250 mm]. The HPLC purity was more than 95% purity. High-resolution mass spectrometry spectra were obtained using fast atom bombardment

(FAB) and electrospray ionization (ESI) methods. Silica gel 60 (230–400 mesh) was used for flash column chromatography, and all solvents were purified and dried before use using standard techniques. Commercially available materials were used without purification unless otherwise stated.

Synthesis and Characterization of the Compounds.

The compound **5d** was synthesized in the previous paper through the intermediates **6–10**, **11b**.[11] The glycosylic donor **16**[26] and the diiodinated purine **17d**[23] were prepared by a known procedure.

(2R,3R,4R)-2-(6-Chloro-8-(furan-2-yl)-2-(hex-1-yn-1-yl)-9H-purin-9-yl)tetrahydrofuran-3,4-diol (11a). Stille Coupling.—To a solution of **10** (530 mg, 0.77 mmol) in anhydrous THF (38 mL) were added 2-(tributylstannyl)furan (0.48 mL, 1.53 mmol) and bis-(triphenylphosphine)palladium(II) dichloride (107 mg, 0.15 mmol) at room temperature under N_2. After being refluxed with stirring for 1 h, the reaction mixture was cooled to room temperature and evaporated. The residue was purified by column chromatography (silica gel, hexane/EtOAc, 30/1 to 15/1) to give the intermediate.

TBS Deprotection.—To a cooled (0 °C) solution of the above-generated intermediate in anhydrous THF (30 mL) were dropwise added triethylamine (0.50 mL, 3.83 mmol) and trimethylamine-trihydrofluoride (0.68 mL, 3.83 mmol) at room temperature under N_2. After being stirred at room temperature for 15 h, the reaction mixture was evaporated. The residue was purified by column chromatography (silica gel, hexane/EtOAc, 1/1) to give **11a** (130 mg, 42%) as white solid: mp 184 °C; $[\alpha]_D^{25} = -34.47$ (*c* 0.11, MeOH); UV (MeOH) λ_{max} 225, 239, 331 nm; ^{1}H NMR (400 MHz, MeOD) δ 7.93 (dd, *J* = 1.6, 0.8 Hz, 1H), 7.49 (dd, *J* = 4.0, 1.2 Hz, 1H), 6.77 (dd, *J* = 3.6, 1.6 Hz, 1H), 6.52 (d, *J* = 6.4 Hz, 1H), 5.40 (dd, *J* = 6.4, 4.8 Hz, 1H), 4.68 (dd, *J* = 9.6, 3.2 Hz, 1H), 4.50–4.54 (m, 1H), 4.03 (dd, *J* = 9.6, 1.6 Hz, 1H), 2.51 (t, *J* = 6.8 Hz, 2H), 1.63–1.69 (m, 2H), 1.50–1.59 (m, 2H), 0.99 (t, *J* = 7.2 Hz, 3H); ^{13}C NMR (100 MHz, MeOD): δ 154.9, 150.9, 150.2, 148.9, 147.3, 144.9, 132.7, 119.2, 114.4, 93.0, 92.2, 81.4, 77.2, 76.2, 73.7, 32.1, 23.9, 20.3, 14.7; HRMS (FAB): found 403.1165 [calcd for $C_{19}H_{20}ClN_4O_4^+$ $(M + H)^+$ 403.1173]; Anal. Calcd for $C_{19}H_{19}ClN_4O_4$: C, 56.65; H, 4.75; N, 13.91. Found: C, 56.91; H, 4.35; N, 13.77.

General Procedure for N^6-Amination for the Preparation of 5a–5f.—To a solution of **11a** or **11b** (1.00 equiv) in EtOH (0.20 M) or *t*-BuOH (0.20 M) were dropwise added appropriate amines (1.50 equiv to excess) at room temperature under N_2. After being stirred at the provided temperature for 12–24 h, the reaction mixture was evaporated. The residue was purified by silica gel column chromatography (CH_2Cl_2/MeOH, 20/1) to give **5a–5f**.

(2R,3R,4R)-2-(6-Amino-8-(furan-2-yl)-2-(hex-1-yn-1-yl)-9H-purin-9-yl)tetrahydrofuran-3,4-diol (5a).—11a was dissolved in NH_3/*t*-BuOH (0.20 M) and stirred for 12 h at 100 °C in a steel bomb. Yield = 78%; white solid; mp 194 °C; $[\alpha]_D^{25} = 15.64$ (*c* 2.16, MeOH); UV (MeOH) λ_{max} 237, 318 nm; ^{1}H NMR (400 MHz, MeOD): δ 7.82 (dd, *J* = 1.6, 0.4 Hz, 1H), 7.19 (dd, *J* = 3.4, 0.4 Hz, 1H), 6.70 (dd, *J* = 3.5, 1.7 Hz, 1H), 6.31 (d, *J* = 6.3 Hz, 1H), 5.44 (dd, *J* = 6.2, 4.8 Hz, 1H), 4.63 (dd, *J* = 9.6, 3.5 Hz, 1H), 4.47–4.48

(m, 1H), 3.98 (dd, J = 9.6, 1.3 Hz, 1H), 2.44 (t, J = 7.1 Hz, 2H), 1.60–1.63 (m, 2H), 1.49–1.54 (m, 2H), 0.97 (t, J = 7.3 Hz, 3H); ^{13}C NMR (100 MHz, MeOD): δ 156.7, 152.0, 147.7, 146.7, 144.8, 144.7, 119.8, 115.5, 113.1, 91.4, 88.1, 81.6, 76.1, 75.0, 72.9, 31.5, 23.1, 19.4, 13.9; HRMS (FAB): found 384.1666 [calcd for $C_{19}H_{22}N_5O_4^+$ $(M + H)^+$ 384.1672]; Anal. Calcd for $C_{19}H_{21}N_5O_4$: C, 59.52; H, 5.52; N, 18.27. Found: C, 59.21; H, 5.32; N, 18.56.

(2R,3R,4R)-2-(8-(Furan-2-yl)-2-(hex-1-yn-1-yl)-6-(methylamino)-9H-purin-9-yl)tetrahydrofuran-3,4-diol (5b).—11a and methylamine hydrochloride (1.50 equiv) were dissolved in EtOH (0.20 M) and stirred for 24 h at room temperature. Yield = 80%; white solid; mp 201 °C; $[\alpha]_D^{25} = -43.62$ (c 0.09, MeOH); UV (MeOH) λ_{max} 244, 325 nm; ^{1}H NMR (800 MHz, DMSO-d_6): δ 7.99 (d, J = 0.8 Hz, 1H), 7.97 (br s, 1H), 7.09 (d, J = 3.4 Hz, 1H), 6.76 (dd, J = 3.0, 1.5 Hz, 1H), 6.11 (d, J = 6.6 Hz, 1H), 5.43 (d, J = 6.5 Hz, 1H), 5.20 (d, J = 3.8 Hz, 1H), 5.17 (q, J = 12.1, 5.5 Hz, 1H), 4.43 (dd, J = 9.2, 3.2 Hz, 1H), 4.30 (d, J = 2.9 Hz, 1H), 3.84 (d, J = 9.2 Hz, 1H), 2.94 (br s, 3H), 2.44 (t, J = 7.0 Hz, 2H), 1.51–1.57 (m, 2H), 1.41–1.47 (m, 2H), 0.92 (t, J = 7.2 Hz, 3H); ^{13}C NMR (200 MHz, DMSO-d_6): δ 154.2, 149.7, 145.7, 145.3, 130.8, 130.0, 129.6, 128.2, 119.0, 88.8, 85.6, 81.8, 74.2, 72.5, 70.5, 29.9, 27.0, 21.5, 17.9, 13.4; HRMS (FAB): found 398.1817 [calcd for $C_{20}H_{24}N_5O_4^+$ $(M + H)^+$ 398.1817]; Anal. Calcd for $C_{20}H_{23}N_5O_4$: C, 60.44; H, 5.83; N, 17.62. Found: C, 60.84; H, 5.45; N, 17.35.

(2R,3R,4R)-2-(8-(Furan-2-yl)-2-(hex-1-yn-1-yl)-6-((3-iodobenzyl)-amino)-9H-purin-9-yl)tetrahydrofuran-3,4-diol (5c).—11a and 3-iodobenzylamine hydrochloride (1.50 equiv) were dissolved in EtOH (0.20 M) and stirred for 24 h at room temperature. Yield = 68%; pale yellow solid; mp 215 °C; $[\alpha]_D^{25} = 233.70$ (c 0.055, MeOH); UV (MeOH) λ_{max} 229, 325 nm; ^{1}H NMR (400 MHz, MeOD): δ 7.81–7.82 (m, 2H), 7.61 (d, J = 8.0 Hz, 1H), 7.42 (dd, J = 7.6, 0.4 Hz, 1H), 7.19 (dd, J = 3.2, 0.4 Hz, 1H), 7.10 (t, J = 7.6 Hz, 1H), 6.70 (dd, J = 3.6, 1.6 Hz, 1H), 6.33 (d, J = 6.8 Hz, 1H), 5.46 (dd, J = 6.4, 4.8, Hz, 1H), 4.77 (br s, 2H), 4.65 (dd, J = 9.6, 3.6 Hz, 1H), 4.48–4.50 (m, 1H), 3.99 (dd, J = 9.6, 1.2 Hz, 1H), 2.46 (t, J = 7.2 Hz, 2H), 1.60–1.66 (m, 2H), 1.51–1.56 (m, 2H), 0.99 (t, J = 7.2 Hz, 3H); ^{13}C NMR (150 MHz, DMSO-d_6): δ 150.3, 145.59, 145.54, 145.52, 143.3, 142.3, 142.1, 135.9, 135.3, 130.4, 126.71, 126.73, 113.7, 112.1, 94.6, 89.1, 86.0, 74.3, 73.0, 70.5, 40.0, 29.8, 27.8, 21.4, 17.9, 13.4; HRMS (FAB): found 600.1109 [calcd for $C_{26}H_{27}IN_5O_4^+$ $(M + H)^+$ 600.1108]; Anal. Calcd for $C_{26}H_{26}IN_5O_4$: C, 52.10; H, 4.37; N, 11.68. Found: C, 52.15; H, 4.32; N, 11.70.

(2R,3R,4R)-2-(6-Amino-2-(hex-1-yn-1-yl)-8-(thiophen-2-yl)-9H-purin-9-yl)tetrahydrofuran-3,4-diol (5d).[11]—The compound was synthesized by the reported procedure. HPLC purity: 98.73%.

(2R,3R,4R)-2-(2-(Hex-1-yn-1-yl)-6-(methylamino)-8-(thiophen-2-yl)-9H-purin-9-yl)tetrahydrofuran-3,4-diol (5e).—11b and methylamine hydrochloride (1.50 equiv) were dissolved in EtOH (0.20 M) and stirred for 24 h at room temperature. Yield = 76%; white solid; mp 216 °C; $[\alpha]_D^{25} = 170.00$ (c 0.01, MeOH); UV (MeOH) λ_{max} 239, 325 nm; ^{1}H NMR (400 MHz, MeOD): δ 7.71 (dd, J = 5.1, 0.9 Hz, 1H), 7.65 (dd, J = 3.6, 0.9 Hz, 1H), 7.23 (dd, J = 5.0, 3.6 Hz, 1H), 6.11 (d, J = 6.4

Hz, 1H), 5.50 (dd, J = 6.3, 4.8 Hz, 1H), 4.63 (dd, J = 9.6, 3.5 Hz, 1H), 4.46 (t, J = 4.6 Hz, 1H), 3.97 (dd, J = 6.0, 1.2 Hz, 1H), 3.08 (br s, 3H), 2.45 (t, J = 7.2 Hz, 2H), 1.61–1.65 (m, 2H), 1.50–1.55 (m, 2H), 0.98 (t, J = 7.3 Hz, 3H); ^{13}C NMR (200 MHz, DMSO-d_6): δ 154.2, 149.7, 145.7, 145.3, 130.8, 130.0, 129.6, 128.2, 119.0, 88.8 (d, J = 7.9 Hz), 85.6, 81.8, 79.1, 74.2 (d, J = 10.5 Hz), 72.6 (d, J = 20.9 Hz), 70.5 (d, J = 21.0 Hz), 29.9, 21.5, 17.9, 13.4; HRMS (FAB): found 414.1605 [calcd for $C_{20}H_{24}N_5O_3S^+$ $(M + H)^+$ 414.1600]; Anal. Calcd for $C_{20}H_{23}N_5O_3S$: C, 58.09; H, 5.61; N, 16.94. Found: C, 57.99; H, 5.86; N, 16.67.

(2R,3R,4R)-2-(2-(Hex-1-yn-1-yl)-6-((3-iodobenzyl)amino)-8-(thiophen-2-yl)-9H-purin-9-yl)tetrahydrofuran-3,4-diol (5f).—11b and 3-iodobenzylamine hydrochloride (1.50 equiv) were dissolved in EtOH (0.20 M) and stirred for 24 h at room temperature. Yield = 78%; white solid; mp 225 °C; $[\alpha]_D^{25}$ = 285.26 (c 0.06, MeOH); UV (MeOH) λ_{max} 231, 326 nm; ^{1}H NMR (400 MHz, DMSO-d_6): δ 8.55 (br s, 1H), 7.88 (dd, J = 5.1, 0.7 Hz, 1H), 7.74 (s, 1H), 7.58–7.60 (m, 2H), 7.35 (d, J = 6.4 Hz, 1H), 7.29 (dd, J = 4.8, 3.7 Hz, 1H), 7.11 (t, J = 7.7 Hz, 1H), 5.97 (d, J = 6.8 Hz, 1H), 5.51 (d, J = 6.5 Hz, 1H), 5.22–5.24 (m, 2H), 4.41 (dd, J = 9.3, 3.3 Hz, 1H), 3.83 (d, J = 8.9 Hz, 1H), 2.42 (t, J = 7.1 Hz, 2H), 1.52–1.56 (m, 2H), 1.42–1.46 (m, 2H), 0.92 (t, J = 7.3 Hz, 3H); ^{13}C NMR (100 MHz, DMSO-d_6): δ 153.6, 150.2, 145.8, 145.5, 142.5, 136.1, 135.4, 130.8, 130.5, 130.2, 129.8, 128.3, 126.8, 118.9, 94.7, 89.0, 81.8, 74.4, 70.6, 42.3, 29.9, 21.5, 18.0, 13.5; HRMS (FAB): found 616.0887 [calcd for $C_{26}H_{27}IN_5O_3S^+$ $(M + H)^+$ 616.0879]; Anal. Calcd for $C_{26}H_{26}IN_5O_3S$: C, 50.74; H, 4.26; N, 11.38. Found: C, 50.75; H, 4.30; N, 11.15.

2,6-Dichloro-8-iodo-9-(tetrahydro-2H-pyran-2-yl)-9H-purine (18).—To a cooled (−78 °C) solution of **17b** (1.27 g, 4.65 mmol) in anhydrous THF (30 mL) was dropwise added LDA (14.0 mL, 1.0 M in THF/hexanes, 14.0 mmol) under N_2, and the reaction mixture was stirred at the same temperature for 1 h. After adding iodine (5.90 g, 23.25 mmol) in THF (10 mL), the reaction mixture was stirred for 1 h. The reaction mixture was quenched with saturated aqueous $Na_2S_2O_3$ (50 mL), diluted with EtOAc (50 mL). The layers were separated, and the aqueous layer was extracted with EtOAc (2 × 50 mL). The combined organic layers were washed successively with H_2O and saturated brine, dried over anhydrous $MgSO_4$, filtered, and evaporated. The residue was purified by column chromatography (silica gel, hexanes/EtOAc, 2/1) to give **18** (1.50 g, 81%) as a brown solid: ^{1}H NMR (800 MHz, $CDCl_3$): δ 5.65 (dd, J = 11.6, 2.4 Hz, 1H), 4.16–4.20 (m, 1H), 3.72 (td, J = 11.6, 2.0 Hz, 1H), 3.03 (ddd, J = 24.0, 12.8, 4.4 Hz, 1H), 2.11–2.19 (m, 1H), 1.57–1.93 (m, 4H); ^{13}C NMR (200 MHz, $CDCl_3$): δ 153.4, 152.6, 150.0, 133.2, 106.4, 86.8, 69.2, 28.7, 24.4, 23.1; HRMS (FAB): found 398.9273 [calcd for $C_{10}H_{10}Cl_2IN_4O^+$ $(M + H)^+$ 398.9283]; Anal. Calcd for $C_{10}H_9Cl_2IN_4O$: C, 30.10; H, 2.27; N, 14.04. Found: C, 30.37; H, 1.91; N, 14.01.

2,6-Dichloro-8-iodopurine (19).—To a solution of **18** (3.0 g, 7.52 mmol) in anhydrous EtOH (50.0 mL, 0.15 M) was added PPTS (378 mg, 1.50 mmol) at room temperature under N_2. After being heated at 60 °C for 6 h, the reaction mixture was quenched with triethylamine (1.0 mL) and evaporated. The residue was purified by column chromatography (silica gel, hexanes/EtOAc, 1/1) to give **19** (2.25 g, 95%) as a yellow solid: ^{13}C NMR (200 MHz, MeOD): δ 163.1, 152.6, 147.0, 134.2, 115.1; HRMS (FAB): found 314.8683 [calcd

for $C_5H_2Cl_2IN4^+$ $(M + H)^+$ 314.8683]; Anal. Calcd for $C_5HCl_2IN_4$: C, 19.07; H, 0.32; N, 17.79. Found: C, 19.07; H, 0.31; N, 17.71.

9-((2R,3R,4S)-3,4-Bis((tert-butyldimethylsilyl)oxy)-tetrahydrothiophen-2-yl)-6-chloro-2,8-diiodo-9H-purine (20).—To a stirred suspension of 2-chloro-8-iodo-6-chloropurine (**17d**) (581 mg, 1.84 mmol) in CH_3CN (10.0 mL) was dropwise added BSA (2.40 mL, 9.83 mmol) at room temperature under N_2, and the mixture was heated at 60 °C until obtaining clear brown solution. To the reaction mixture was quickly added **16** (500 mg, 1.23 mmol) in CH_3CN (5.0 mL) and TMSOTf (0.22 mL, 1.23 mmol), and the mixture was stirred at 75 °C for 1.5 h. The reaction mixture was cooled to room temperature, quenched with saturated $NaHCO_3$ solution (30 mL), and diluted with EtOAc (30 mL). The layers were separated, and the aqueous layer was extracted with EtOAc (3 × 30 mL). The combined organic layers were washed successively with H_2O (50 mL), dried over anhydrous $MgSO_4$, filtered, and evaporated. The residue was purified by column chromatography (silica gel, hexanes/EtOAc, 30/1) to give **20** (569.0 mg, 41%) as brown syrup: ^1H NMR (400 MHz, $CDCl_3$): δ 6.01 (d, J = 7.2 Hz, 1H), 5.26 (dd, J = 7.2, 2.8 Hz, 1H), 4.55 (dd, J = 5.6, 2.4 Hz, 1H), 3.54 (dd, J = 11.2, 3.2 Hz, 1H), 2.86 (dd, J = 11.2, 2.4 Hz, 1H), 0.98 (s, 9H), 0.74 (s, 9H), 0.17 (s, 3H), 0.16 (s, 3H); ^{13}C NMR (100 MHz, MeOD): δ 154.7, 149.9, 136.2, 118.2, 113.3, 95.1, 76.9, 76.7, 75.0, 27.2, 27.1, 19.8, 19.5; HRMS (FAB): found 752.9854 [calcd for $C_{21}H_{36}ClI_2N_4O_2SSi_2^+$ $(M + H)^+$ 752.9876]; Anal. Calcd for $C_{21}H_{35}ClI_2N_4O_2SSi_2$: C, 33.49; H, 4.68; N, 7.44. Found: C, 33.87; H, 4.31; N, 7.11.

General Procedure for Stille Coupling for the Preparation of 21a and 21b.—To a stirred solution of **20** (1.00 equiv) in DMF/toluene (v/v = 1/1, 0.040 M) was added bis(dibenzylideneacetone)-palladium(0) (0.10 equiv), followed by 2-(tributylstannyl)furan (1.05 equiv, for **21a**), or 2-(tributylstannyl)thiophene (1.05 equiv, for **21b**) dropwise at room temperature under N_2. After being stirred for 9 h (for **21a**) or 23 h (for **21b**) at the same condition, the reaction mixture was quenched with saturated $NaHCO_3$ solution and diluted with Et_2O. The layers were separated, and the aqueous layer was extracted with Et_2O. The combined organic layers were washed successively with H_2O and saturated brine, dried over anhydrous $MgSO_4$, filtered, and evaporated. The residue was purified by column chromatography to give **21a**, or **21b**.

9-((2R,3R,4S)-3,4-Bis((tert-butyldimethylsilyl)oxy)-tetrahydrothiophen-2-yl)-6-chloro-8-(furan-2-yl)-2-iodo-9H-purine (21a).—21a was isolated by column chromatography (silica gel, hexanes/EtOAc, 100/3 to 25/2). Yield = 69%; yellow oil; $[\alpha]_D^{21} = -73.9$ (c 1.21, MeOH); UV (MeOH) λ_{max} 326 nm; ^1H NMR (400 MHz, MeOD): δ 7.89 (dd, J = 0.9, 0.7 Hz, 1H), 7.46 (dd, J = 0.9, 2.8 Hz, 1H), 6.79 (dd, J = 3.6, 1.6 Hz, 1H), 6.72 (d, J = 7.8 Hz, 1H), 5.44 (dd, J = 7.8, 2.7 Hz, 1H), 4.61 (q, J = 2.4 Hz, 1H), 3.61 (dd, J = 11.2, 3.0, Hz, 1H), 2.87 (dd, J = 11.2, 2.1 Hz, 1H), 1.00 (s, 9h), 0.63 (s, 9H), 0.20 (s, 3H), 0.17 (s, 3H), −0.07 (s, 3H), −0.54 (s, 3H); ^{13}C NMR (200 MHz, MeOD): δ 155.4, 150.8, 149.7, 148.8, 145.0, 134.0, 119.3, 117.2, 114.5, 80.0, 76.2, 66.5, 37.6, 27.1, 26.8, 19.8, 19.4, −3.4, −3.4, −3.5, −4.6. HRMS (ESI): found 693.1027 [calcd for $C_{25}H_{38}ClIN_4O_3SSi_2^+$ $(M + H)^+$ 692.0936].

9-((2R,3R,4S)-3,4-Bis((tert-butyldimethylsilyl)oxy)-tetrahydrothiophen-2-yl)-6-chloro-2-iodo-8-(thiophen-2-yl)-9H-purine (21b).—21b was isolated by column chromatography (silica gel, hexanes/EtOAc, 40/1). Yield = 44%; yellow oil; $[\alpha]_D^{21} = -91.9$ (c 0.18, MeOH); UV (MeOH) λ_{max} 330 nm; ^{1}H NMR (400 MHz, MeOD): δ 7.91 (dd, J = 5.1, 0.9 Hz, 1H), 7.81 (dd, J = 3.7, 0.9 Hz, 1H), 7.29 (dd, J = 5.1, 3.7 Hz, 1H), 6.43 (d, J = 8.3 Hz, 1H), 5.53 (dd, J = 8.3, 2.8 Hz, 1H), 4.60 (q, J = 2.5 Hz, 1H), 3.60 (dd, J = 11.5, 2.8 Hz, 1H), 2.87 (dd, J = 11.5, 1.8 Hz, 1H), 0.94 (s, 9H), 0.63 (s, 9H), 0.19 (s, 3H), 0.15 (s, 3H), −0.06 (s, 3H), −0.44 (s, 3H); ^{13}C NMR (200 MHz, MeOD): δ 153.66, 151.63, 149.67, 132.37, 131.48, 131.33, 129.33, 128.28, 115.19, 77.73, 73.98, 64.29, 36.03, 25.83, 25.68, 18.17, 17.93, −4.20, −4.36, −4.47, −5.14. HRMS (ESI): found 709.0781 [calcd for $C_{25}H_{38}ClIN_4O_2S_2Si_2^+$ $(M + H)^+$ 709.0781].

General Procedure for Sonogashira Coupling and Desilylation for the Preparation of 22a and 22b. Sonogashira Coupling.—To a stirred solution of **21a** (1.00 equiv, for **22a**) or **21b** (1.00 equiv, for **22b**) in DMF (0.10 M) were added bis(triphenylphosphine)-palladium(II) dichloride (0.10 equiv), copper(I) iodide (0.20 equiv), and cesium carbonate (1.5 equiv), followed by 1-hexyne (1.05 equiv) dropwise at room temperature under N_2. After being stirred for 14 h (for **22a**) or 16 h (for **22b**) at the same condition, the reaction mixture was quenched with H_2O and diluted with Et_2O. The layers were separated, and the aqueous layer was extracted with Et_2O. The combined organic layers were washed successively with H_2O and saturated brine, dried over anhydrous $MgSO_4$, filtered, and evaporated. The residue was purified by column chromatography to give the coupling products.

TBS Deprotection.—To a solution of coupling product (1.00 equiv) in THF (0.10 M) was added the mixture of tetrabutylammoniumfluoride (1.0 M in THF) and acetic acid (v/v = 10/1, 2.50 equiv) at room temperature under N_2. After being stirred for 16 h (for **22a**) or 12 h (for **22b**) at 50 °C under N_2, the reaction mixture was quenched by H_2O, and diluted with EtOAc. The layers were separated, and the aqueous layer was extracted with EtOAc. The combined organic layers were dried over anhydrous $MgSO_4$, filtered, and evaporated. The residue was purified by column chromatography to give **22a** or **22b**.

(2R,3R,4S)-2-(6-Chloro-8-(furan-2-yl)-2-(hex-1-yn-1-yl)-9H-purin-9-yl)tetrahydrothiophene-3,4-diol (22a). Sonogashira Coupling.—The coupling product was isolated by column chromatography (silica gel, hexanes/EtOAc, 100/3 to 50/2). Yield = 73%; yellow oil; $[\alpha]_D^{21} = -56.2$ (c 0.84, MeOH); UV (MeOH) λ_{max} 330 nm; ^{1}H NMR (400 MHz, MeOD): δ 7.89 (d, J = 1.8 Hz, 1H), 7.46 (dd, J = 3.6, 0.8 Hz, 1H), 6.79 (dd, J = 3.4, 1.6 Hz, 1H), 6.72 (d, J = 7.8 Hz, 1H), 5.48 (dd, J = 7.5, 3.0 Hz, 1H), 4.66 (q, J = 2.6 Hz, 1H), 3.63 (dd, J = 11.2, 3.0 Hz, 1H), 2.88 (dd, J = 11.4, 2.3 Hz, 1H), 2.53 (t, J = 6.9 Hz, 2H), 1.64–1.71 (m, 2H), 1.51–1.60 (m, 2H), 1.00 (s, 9H), 1.00 (t, J = 7.2 Hz, 3H), 0.20 (s, 3H), 0.17 (s, 3H), −0.07 (s, 3H), −0.55 (s, 3H); ^{13}C NMR (200 MHz, MeOD): δ 154.9, 151.2, 150.4, 148.7, 147.0, 145.2, 133.0, 119.1, 114.5, 92.5, 81.5, 79.9, 76.3, 66.5, 37.5, 32.1, 27.1, 26.8, 23.9, 20.4, 19.8, 19.4, 14.8, −3.4, −3.5, −3.6, −4.7. HRMS (ESI): found 647.2664 [calcd for $C_{31}H_{48}ClN_4O_3SSi_2^+$ $(M + H)^+$ 646.2596].

TBS Deprotection.—22a was isolated by column chromatography (silica gel, CH_2Cl_2/MeOH, 50/1). Yield = 94%; yellow solid; $[\alpha]_D^{21} = -110.8$ (c 0.13, MeOH); UV (MeOH) λ_{max} 330 nm; ^{1}H NMR (400 MHz, MeOD): δ 7.95 (d, J = 1.4 Hz, 1H), 7.51 (d, J = 3.7 Hz, 1H), 6.79 (dd, J = 3.7, 1.8 Hz, 1H), 6.61 (d, J = 7.8 Hz, 1H), 5.61 (dd, J = 7.8, 3.7 Hz, 1H), 4.59 (q, J = 2.8 Hz, 1H), 3.74 (dd, J = 11.5, 3.2 Hz, 1H), 2.97 (dd, J = 11.5, 1.8 Hz, 1H), 2.52 (t, J = 6.9 Hz, 2H), 1.63–1.70 (m, 2H), 1.50–1.60 (m, 2H), 1.00 (t, J = 7.1 Hz, 3H); ^{13}C NMR (200 MHz, MeOD): δ 154.9, 151.0, 150.4, 148.8, 146.9, 145.0, 133.0, 118.9, 114.5, 92.2, 81.5, 79.2, 75.5, 67.7, 37.8, 32.2, 23.9, 20.3, 14.7. HRMS (FAB): found 419.0944 [calcd for $C_{19}H_{20}ClN_4O_3S^+$ $(M + H)^+$ 419.0945].

(2R,3R,4S)-2-(6-Chloro-2-(hex-1-yn-1-yl)-8-(thiophen-2-yl)-9H-purin-9-yl)tetrahydro-thiophene-3,4-diol (22b). Sonogashira Coupling.— The coupling product was isolated by column chromatography (silica gel, hexanes/EtOAc, 100/3 to 50/2). Yield = 64%; colorless oil; $[\alpha]_D^{21} = -56.2$ (c 0.84, MeOH); ^{1}H NMR (400 MHz, MeOD): δ 7.91 (dd, J = 5.3, 1.1 Hz, 1H), 7.83 (dd, J = 3.7, 0.9 Hz, 1H), 7.30 (dd, J = 5.3, 3.9 Hz, 1H), 6.44 (d, J = 8.2 Hz, 1H), 5.57 (dd, J = 8.0, 3.0 Hz, 1H), 4.64 (q, J = 2.4 Hz, 1H), 3.64 (dd, J = 11.4, 3.2 Hz, 1H), 2.88 (dd, J = 11.4, 2.3 Hz, 1H), 2.54 (t, J = 7.1 Hz, 2H), 1.64–1.72 (m, 2H), 1.51–1.60 (m, 2H), 1.01 (t, J = 7.3 Hz, 3H), 0.94 (s, 9H), 0.63 (s, 9H), 0.19 (s, 3H), 0.15 (s, 3H), −0.06 (s, 3H), −0.47 (s, 3H); ^{13}C NMR (200 MHz, MeOD): δ 155.1, 154.7, 151.2, 147.0, 133.8, 133.3, 132.9, 131.1, 130.1, 92.5, 81.5, 79.5, 75.9, 66.3, 37.2, 32.1, 27.1, 26.8, 23.9, 20.3, 19.7, 19.4, 14.7, −3.4, −3.4, −3.6, −4.5. HRMS (ESI): found 663.2450 [calcd for $C_{31}H_{48}ClN_4O_2S_2Si_2^+$ $(M + H)^+$ 663.2440].

TBS Deprotection.—22b was isolated by column chromatography (silica gel, CH_2Cl_2/MeOH, 50/1). Yield = 73%; white solid; $[\alpha]_D^{21} = -94.8$ (c 0.52, MeOH); UV (MeOH) λ_{max} 326 nm; ^{1}H NMR (400 MHz, MeOD): δ 7.90 (dd, J = 3.7, 0.9 Hz, 1H), 7.88 (dd, J = 5.1, 1.4 Hz, 1H), 7.32 (dd, J = 5.1, 3.7 Hz, 1H), 6.33 (d, J = 7.8 Hz, 1H), 5.65 (q, J = 3.8 Hz, 1H), 4.56 (td, J = 3.4, 1.7 Hz, 1H), 3.73 (dd, J = 11.5, 3.7 Hz, 1H), 2.96 (dd, J = 11.5, 1.8 Hz, 1H), 2.52 (t, J = 6.9 Hz, 2H), 1.63–1.70 (m, 2H), 1.50–1.59 (m, 2H), 1.00 (t, J = 7.1 Hz, 3H); ^{13}C NMR (200 MHz, MeOD): δ 155.2, 154.6, 150.9, 146.9, 133.7, 133.4, 132.9, 131.2, 130.3, 92.1, 81.5, 78.9, 75.3, 67.5, 37.6, 32.2, 23.9, 20.3, 14.7. HRMS (FAB): found 435.0717 [calcd for $C_{19}H_{20}ClN_4O_3S^+$ $(M + H)^+$ 435.0711].

General Procedure for N^6-Amination for the Preparation of 5g–5l.—To a solution of **22a** or **22b** (1.00 equiv) in EtOH (0.20 M) or t-BuOH (0.20 M) were dropwise added appropriate amines (1.50 equiv to excess) at room temperature under N_2. After being stirred at the provided temperature for 12–28 h, the reaction mixture was evaporated. The residue was purified by silica gel column chromatography (CH_2Cl_2/MeOH, 20/1) to give **5g–5l**.

(2R,3R,4S)-2-(6-Amino-8-(furan-2-yl)-2-(hex-1-yn-1-yl)-9H-purin-9-yl)tetrahydro-thiophene-3,4-diol (5g).—22a was dissolved in NH_3/t-BuOH (0.20 M) and stirred for 15 h at 100 °C in a steel bomb. Yield = 44%; white solid; mp 220 °C; $[\alpha]_D^{21} = -205.2$ (c 0.05, MeOH); UV (MeOH) λ_{max} 238, 320 nm; ^{1}H NMR (400 MHz, MeOD): δ 7.85 (d, J = 1.8 Hz, 1H), 7.23 (d, J = 3.2 Hz, 1H), 6.72 (q, J = 1.7 Hz, 1H), 6.41 (d, J = 7.8 Hz, 1H), 5.65 (dd, J = 3.2, 1.8 Hz, 1H), 4.56 (td, J = 3.4, 1.8 Hz, 1H), 3.73 (dd, J = 11.4, 3.7 Hz, 1H),

2.92 (dd, J = 11.4, 1.8 Hz, 1H), 2.46 (t, J = 6.9 Hz, 2H), 1.60–1.68 (m, 2H), 1.49–1.58 (m, 2H), 0.99 (t, J = 7.3 Hz, 3H); ^{13}C NMR (100 MHz, DMSO-d_6): δ 155.68, 150.44, 145.49, 145.48, 143.53, 142.14, 118.89, 113.36, 112.20, 85.70, 81.64, 75.98, 72.14, 63.88, 35.65, 29.93, 21.51, 17.97, 13.48. HRMS (FAB): found 400.1443 [calcd for $C_{19}H_{22}N_5O_3S^+$ (M + H)$^+$ 400.1441]; HPLC purity: 99.50%.

(2R,3R,4S)-2-(8-(Furan-2-yl)-2-(hex-1-yn-1-yl)-6-(methylamino)-9H-purin-9-yl)tetrahydrothiophene-3,4-diol (5h).—22a and methylamine hydrochloride (1.50 equiv) were dissolved in EtOH (0.20 M) and stirred for 23 h at 50 °C. Yield = 65%; white solid; mp 210 °C; $[\alpha]_D^{21} = -135.8$ (c 0.06, MeOH); UV (MeOH) λ_{max} 244, 326 nm; ^{1}H NMR (400 MHz, MeOD): δ 7.82 (s, 1H), 7.19 (d, J = 3.7 Hz, 1H), 6.70 (dd, J = 3.4, 1.6 Hz, 1H), 6.40 (d, J = 7.8 Hz, 1H), 5.65 (dd, J = 7.6, 3.4 Hz, 1H), 4.56 (q, J = 2.8 Hz, 1H), 3.73 (dd, J = 11.5, 3.7 Hz, 1H), 3.10 (s, 3H), 2.92 (dd, J = 11.5, 1.4 Hz, 1H), 2.47 (t, J = 6.9 Hz, 2H), 1.62–1.69 (m, 2H), 1.49–1.59 (m, 2H), 0.99 (t, J = 7.4 Hz, 3H); ^{13}C NMR (200 MHz, MeOD): δ 157.08, 148.45, 147.27, 145.83, 144.92, 121.48, 115.62, 113.89, 88.49, 82.80, 79.02, 75.52, 66.78, 37.49, 32.38, 23.94, 20.35, 14.76. HRMS (FAB): found 414.1600 [calcd for $C_{20}H_{24}N_5O_3S^+$ (M + H)$^+$ 414.1607]; HPLC purity: 99.00%.

(2R,3R,4S)-2-(8-(Furan-2-yl)-2-(hex-1-yn-1-yl)-6-((3-iodobenzyl)-amino)-9H-purin-9-yl)tetrahydrothiophene-3,4-diol (5i).—22a and 3-iodobenzylamine hydrochloride (1.50 equiv) were dissolved in EtOH (0.20 M) and stirred for 24 h at 50 °C. Yield = 79%; white solid; mp 238 °C; $[\alpha]_D^{21} = 79.11$ (c 0.07, MeOH); UV (MeOH) λ_{max} 246, 325 nm; ^{1}H NMR (400 MHz, DMSO-d_6): δ 8.62 (s, 1H), 8.03 (d, J = 1.4 Hz, 1H), 7.75 (s, 1H), 7.59 (d, J = 7.8 Hz, 1H), 7.35 (d, J = 7.8 Hz, 1H), 7.14 (d, J = 3.2 Hz, 1H), 7.11 (d, J = 7.8 Hz, 1H), 6.79 (dd, J = 3.2, 1.8 Hz, 1H), 6.20 (d, J = 7.8 Hz, 1H), 5.47 (d, J = 6.4 Hz, 1H), 5.38–5.41 (m, 2H), 4.63 (s, 2H), 4.38 (s, 1H), 3.48 (dd, J = 11.2, 3.4 Hz, 1H), 2.81 (d, J = 10.5 Hz, 1H), 2.44 (t, J = 7.1 Hz, 2H), 1.51–1.59 (m, 2H), 1.40–1.49 (m, 2H), 0.92 (t, J = 7.1 Hz, 3H); ^{13}C NMR (100 MHz, DMSO-d_6): δ 153.75, 149.88, 145.60, 145.33, 143.51, 142.50, 142.26, 136.05, 135.45, 130.51, 126.78, 119.32, 113.51, 112.26, 94.74, 86.10, 81.90, 76.12, 72.15, 63.94, 42.26, 35.69, 29.91, 21.56, 18.06, 13.53. HRMS (FAB): found 616.0879 [calcd for $C_{26}H_{27}IN_5O_3S^+$ (M + H)$^+$ 616.0876]; HPLC purity: 95.75%.

(2R,3R,4S)-2-(6-Amino-2-(hex-1-yn-1-yl)-8-(thiophen-2-yl)-9H-purin-9-yl)tetrahydro-thiophene-3,4-diol (5j).—22b was dissolved in NH_3/t-BuOH (0.20 M) and stirred for 15 h at 100 °C in a steel bomb. Yield = 83%; white solid; mp 197 °C; $[\alpha]_D^{21} = -141.6$ (c 0.15, MeOH); UV (MeOH) λ_{max} 236, 319 nm; ^{1}H NMR (400 MHz, DMSO-d_6): δ 7.88 (d, J = 4.1 Hz, 1H), 7.64 (d, J = 3.2 Hz, 1H), 7.45 (s, 2H), 7.31 (dd, J = 5.1, 3.7 Hz, 1H), 6.05 (d, J = 7.8 Hz, 1H), 5.43–5.49 (d, J = 6.8 Hz, 1H), 5.49 (d, J = 6.8 Hz, 1H), 5.46 (qd, J = 7.2, 2.8 Hz, 1H), 5.35 (d, J = 3.7 Hz, 1H), 4.37 (d, J = 1.8 Hz, 1H), 3.47 (dd, J = 11.0, 3.2 Hz, 1H), 2.80 (d, J = 10.6 Hz, 1H), 2.43 (t, J = 7.1 Hz, 2H), 1.50–1.58 (m, 2H), 1.39–1.48 (m, 2H), 0.92 (t, J = 7.4 Hz, 3H); ^{13}C NMR (200 MHz, DMSO-d_6): δ 155.46, 150.78, 145.56, 145.29, 130.90, 129.99, 128.97, 128.21, 118.73, 85.60, 81.63, 75.58, 71.92, 63.94, 35.56, 29.89, 21.48, 17.94, 13.44. HRMS (FAB): found 416.1219 [calcd for $C_{19}H_{22}N_5O_2S_2^+$ (M + H)$^+$ 416.1215]; HPLC purity: 99.56%.

(2R,3R,4S)-2-(2-(Hex-1-yn-1-yl)-6-(methylamino)-8-(thiophen-2-yl)-9H-purin-9-yl)tetrahydrothiophene-3,4-diol (5k).—22b and methylamine hydrochloride (1.50 equiv) were dissolved in EtOH (0.20 M) and stirred for 28 h at 50 °C. Yield = 61%; white solid; mp 238 °C; $[\alpha]_D^{21}$ = 237.09 (*c* 0.04, DMSO); UV (MeOH) λ_{max} 242, 326 nm; ^{1}H NMR (400 MHz, DMSO-d_6): δ 7.89 (s, 1H), 7.87 (dd, *J* = 5.0, 0.9 Hz, 1H), 7.64 (dd, *J* = 3.7, 0.9 Hz, 1H), 7.31 (dd, *J* = 5.0, 3.7 Hz, 1H), 6.06 (d, *J* = 8.2 Hz, 1H), 5.51 (d, *J* = 6.4 Hz, 1H), 5.42–5.46 (m, 1H), 5.37 (d, *J* = 3.2 Hz, 1H), 4.37 (d, *J* = 1.4 Hz, 1H), 3.48 (dd, *J* = 11.2, 3.4 Hz, 1H), 2.92 (s, 3H), 2.81 (dd, *J* = 11.2, 1.1 Hz, 1H), 2.45 (t, *J* = 7.3 Hz, 2H), 1.53–1.60 (m, 2H), 1.40–1.49 (m, 2H), 0.93 (t, *J* = 7.1 Hz, 3H); ^{13}C NMR (200 MHz, MeOD): δ 154.32, 149.77, 145.37, 145.27, 130.96, 129.96, 128.91, 128.24, 119.31, 85.72, 81.97, 75.70, 71.95, 63.95, 35.59, 29.93, 27.08, 21.59, 18.03, 13.47. HRMS (FAB): found 430.1372 [calcd for $C_{20}H_{24}N_5O_2S_2^+$ (M + H)$^+$ 430.1371]; HPLC purity: 99.17%.

(2R,3R,4S)-2-(2-(Hex-1-yn-1-yl)-6-((3-iodobenzyl)amino)-8-(thiophen-2-yl)-9H-purin-9-yl)tetrahydrothiophene-3,4-diol (5l).—22b and 3-iodobenzylamine hydrochloride (1.50 equiv) were dissolved in EtOH (0.20 M) and stirred for 20 h at 75 °C. Yield = 78%; white solid; mp 236 °C; $[\alpha]_D^{21}$ = 100.99 (*c* 0.11, DMSO); UV (MeOH) λ_{max} 248, 326 nm; ^{1}H NMR (400 MHz, DMSO-d_6): δ 8.53 (s, 1H), 7.89 (d, *J* = 5.0 Hz, 1H), 7.76 (s, 1H), 7.65 (d, *J* = 3.2 Hz, 1H), 7.59 (d, *J* = 7.8 Hz, 1H), 7.36 (d, *J* = 5.5 Hz, 1H), 7.31 (t, *J* = 4.1 Hz, 1H), 7.12 (t, *J* = 7.8 Hz, 1H), 6.07 (d, *J* = 8.2 Hz, 1H), 5.52 (d, *J* = 5.0 Hz, 1H), 5.44 (t, *J* = 3.0 Hz, 1H), 5.38 (s, 1H), 4.62 (s, 2H), 4.37 (s, 1H), 3.47 (dd, *J* = 11.0, 2.7 Hz, 1H), 2.81 (d, *J* = 11.0 Hz, 1H), 2.44 (t, *J* = 7.1 Hz, 2H), 1.52–1.59 (m, 2H), 1.40–1.49 (m, 2H), 0.93 (t, *J* = 7.1 Hz, 3H); ^{13}C NMR (100 MHz, DMSO-d_6): δ 153.59, 150.29, 145.80, 145.23, 142.58, 136.12, 135.49, 130.92, 130.55, 130.21, 129.13, 128.39, 126.87, 119.23, 94.77, 86.12, 81.96, 75.77, 72.01, 64.06, 54.98, 42.32, 35.67, 29.95, 21.62, 18.10, 13.58. HRMS (FAB): found 632.0653 [calcd for $C_{26}H_{27}IN_5O_2S_2^+$ (M + H)$^+$ 632.0651].

9-((2R,3R,4S)-3,4-Bis((tert-butyldimethylsilyl)oxy)-tetrahydrothiophen-2-yl)-6-chloro-2,8-diiodo-9H-purine (23).—To a stirred solution of 2,6-dichloro-8-iodopurine (**19**) (581 mg, 1.84 mmol) in CH_3CN (10.0 mL) was dropwise added BSA (2.4 mL, 9.83 mmol) at room temperature under N_2, and the reaction mixture was heated at 60 °C until obtaining a clear solution. To the reaction mixture was dropwise added **16** (500 mg, 1.23 mmol) in CH_3CN (5.0 mL) and TMSOTf (0.22 mL, 1.23 mmol). After being stirred at 75 °C for 1.5 h, the reaction mixture was cooled to room temperature and evaporated. The residue was purified by column chromatography (silica gel, hexanes/EtOAc, 10/1) to give **23** (400 mg, 54%) as a colorless syrup: $[\alpha]_D^{25}$ = −1.02 (*c* 37.53, MeOH); UV (MeOH) λ_{max} 229, 286 nm; ^{1}H NMR (400 MHz, DMSO-d_6): δ 5.98 (d, *J* = 7.2 Hz, 1H), 5.08 (dd, *J* = 7.2, 2.8 Hz, 1H), 4.64 (dd, *J* = 5.2, 2.8 Hz, 1H), 3.43 (dd, *J* = 11.2, 3.2 Hz, 1H), 2.78 (dd, *J* = 11.6, 2.8 Hz, 1H), 0.91 (s, 9H), 0.62 (s, 9H), 0.11 (s, 3H), 0.09 (s, 3H), −0.1 (s, 3H), −0.53 (s, 3H); ^{13}C NMR (200 MHz, DMSO-d_6): δ 152.9, 150.5, 148.3, 133.5, 128.2, 77.1, 73.3, 66.5, 35.4, 25.6, 25.2, 17.7, 17.3, −4.6, −4.7, −4.7, −5.8; HRMS (FAB): found 661.0459 [calcd for $C_{21}H_{36}Cl_2IN_4O_2SSi_2^+$ (M + H)$^+$ 661.0451]; Anal. Calcd for $C_{21}H_{35}ClI_2N_4O_2SSi_2$: C, 33.49; H, 4.68; N, 7.44. Found: C, 33.11; H, 5.08; N, 7.19.

General Procedure for Stille Coupling for the Preparation of *24a* and 24b.—To a solution of **23** (2.90 g, 4.38 mmol) in anhydrous THF (0.10 M) was added bis(triphenylphosphine)palladium(II) dichloride (0.10 equiv), 2-(tributylstannyl)furan (1.50 equiv, for **24a**), or 2-(tributylstannyl)thiophene (1.50 equiv, for **24b**) at room temperature under N_2. After being heated reflux with stirring for 24 h, the reaction mixture was cooled to room temperature and evaporated. The residue was purified by column chromatography to give **24a** or **24b**.

9-((2R,3R,4S)-3,4-Bis((tert-butyldimethylsilyl)oxy)-tetrahydrothiophen-2-yl)-2,6-dichloro-8-(furan-2-yl)-9H-purine (24a).—24a was isolated by column chromatography (silica gel, hexanes/EtOAc, 20/1). Yield = 71%; colorless oil; $[\alpha]_D^{25} = -25.42$ (*c* 0.045, MeOH); UV (MeOH) λ_{max} 322 nm; ^{1}H NMR (400 MHz, $CDCl_3$): δ 7.66–7.69 (m, 1H), 7.38 (d, *J* = 3.2 Hz, 1H), 6.65–6.66 (m, 2H), 5.32 (dd, *J* = 6.8, 2.8 Hz, 1H), 4.56–4.60 (m, 1H), 3.57 (dd, *J* = 10.8, 3.2 Hz, 1H), 2.86 (dd, *J* = 11.2, 3.2 Hz, 1H), 0.96 (s, 9H), 0.65 (s, 9H), 0.16 (s, 3H), 0.14 (s, 9H), −0.11 (s, 3H), −0.52 (s, 3H); ^{13}C NMR (150 MHz, MeOD): δ 155.3, 152.8, 151.5, 149.7, 148.0, 144.3, 132.6, 118.6, 113.8, 79.3, 75.4, 65.8, 36.8, 26.4, 26.0, 19.0, 18.6, −4.2, −4.2, −4.3, −5.5; HRMS (FAB): found 601.1652 [calcd for $C_{25}H_{39}Cl_2N_4O_3SSi_2^+$ $(M + H)^+$ 601.1651]; Anal. Calcd for $C_{25}H_{38}Cl_2N_4O_3SSi_2$: C, 49.90; H, 6.37; N, 9.31. Found: C, 49.94; H, 6.36; N, 9.37.

9-((2R,3R,4S)-3,4-Bis((tert-butyldimethylsilyl)oxy)-tetrahydrothiophen-2-yl)-2,6-dichloro-8-(thiophen-2-yl)-9H-purine (24b).—24b was isolated by column chromatography (silica gel, hexanes/EtOAc, 40/1). Yield = 56%; colorless oil; $[\alpha]_D^{25} = 66.89$ (*c* 0.10, DMSO); UV (MeOH) λ_{max} 253, 315 nm; ^{1}H NMR (400 MHz, $CDCl_3$): δ 7.77 (d, *J* = 4.4 Hz, 1H), 7.65 (d, *J* = 5.2 Hz, 1H), 7.19 (dd, *J* = 5.2, 4.0 Hz, 1H), 6.40 (d, *J* = 7.6 Hz, 1H), 5.39 (dd, *J* = 7.6, 2.8 Hz, 1H), 4.52–4.56 (m, 1H), 3.58 (dd, *J* = 10.8, 2.4 Hz, 1H), 2.84 (dd, *J* = 10.8, 2.4 Hz, 1H), 0.92 (s, 9H), 0.65 (s, 9H), 0.14 (s, 3H), 0.12 (s, 3H), −0.11 (s, 3H), −0.46 (s, 3H); ^{13}C NMR (150 MHz, $CDCl_3$): δ 154.4, 152.4, 151.9, 151.0, 135.8, 131.5, 131.4, 129.5, 128.3, 77.8, 74.0, 64.4, 36.0, 25.9, 25.7, 18.2, 18.0, −4.2, −4.3, −4.4, −5.2; HRMS (FAB): found 617.1452 [calcd for $C_{25}H_{39}Cl_2N_4O_2S_2Si_2^+$ $(M + H)^+$ 617.1451]; Anal. Calcd for $C_{25}H_{38}Cl_2N_4O_2S_2Si_2$: C, 48.60; H, 6.20; N, 9.07. Found: C, 48.66; H, 6.24; N, 9.02.

General Procedure for Desilylation and N^6-Amination for the Synthesis of *5m–5r*.—To a solution of **24a** or **24b** (1.00 equiv) in anhydrous THF (0.10 M) was dropwise added TBAF (2.50 equiv) at room temperature. The reaction mixture was stirred at the same temperature for 1 h and evaporated. The residue was purified by column chromatography (silica gel, hexanes/EtOAc, 5/1 to 3/1) to give a diol intermediate. To a solution of the diol intermediate (1.00 equiv) in EtOH (0.20 M) or *t*-BuOH (0.20 M) were dropwise added appropriate amines (1.50 equiv to excess) at room temperature under N_2. After being stirred at the provided temperature for 15–24 h, the reaction mixture was evaporated. The residue was purified by silica gel column chromatography (CH_2Cl_2/MeOH, 20/1) to give **5m–5r**.

(2R,3R,4S)-2-(6-Amino-2-chloro-8-(furan-2-yl)-9H-purin-9-yl)-tetrahydrothiophene-3,4-diol (5m).—Yield = 56%; pale yellow solid; mp 241

°C; $[\alpha]_D^{25} = -14.13$ (*c* 0.045, MeOH); UV (MeOH) λ_{max} 242, 305 nm; ^{1}H NMR (400 MHz, MeOD): δ 7.82 (d, *J* = 1.8 Hz, 1H), 7.20 (d, *J* = 2.7 Hz, 1H), 6.70 (dd, *J* = 3.7, 1.8 Hz, 1H), 6.37 (d, *J* = 7.8 Hz, 1H), 5.54 (dd, *J* = 7.3, 3.6 Hz, 1H), 4.54 (dd, *J* = 5.4, 3.6 Hz, 1H), 3.67 (dd, *J* = 11.4, 3.2 Hz, 1H), 2.91 (dd, *J* = 11.4, 1.8 Hz, 1H); ^{13}C NMR (150 MHz, MeOD): δ 158.6, 155.5, 153.5, 147.4, 145.5, 145.2, 120.4, 115.8, 113.9, 79.1, 75.5, 67.0, 37.5; HRMS (FAB): found 354.0416 [calcd for $C_{13}H_{13}ClN_5O_3S^+$ $(M + H)^+$ 354.0428]; Anal. Calcd for $C_{13}H_{12}ClN_5O_3S$: C, 44.13; H, 3.42; N, 19.80. Found: C, 43.91; H, 3.14; N, 19.95.

(2R,3R,4S)-2-(2-Chloro-8-(furan-2-yl)-6-(methylamino)-9H-purin-9-yl)tetrahydrothiophene-3,4-diol (5n).—Yield = 55%; white solid; mp 224 °C; $[\alpha]_D^{25} = -8.10$ (*c* 0.06, MeOH); UV (MeOH) λ_{max} 245, 310 nm; ^{1}H NMR (400 MHz, MeOD): δ 7.80 (d, *J* = 1.9 Hz, 1H), 7.16 (d, *J* = 3.1 Hz, 1H), 6.68 (dd, *J* = 3.7, 1.8 Hz, 1H), 6.36 (d, *J* = 7.3 Hz, 1H), 5.54 (dd, *J* = 7.8, 3.6 Hz, 1H), 4.54 (dd, *J* = 5.0, 3.1 Hz, 1H), 3.67 (dd, *J* = 11.4, 3.6 Hz, 1H), 3.07 (br s, 3H), 2.91 (dd, *J* = 11.4, 2.2 Hz, 1H); ^{13}C NMR (200 MHz, MeOD): δ 157.8, 155.8, 152.3, 147.2, 145.7, 144.6, 121.2, 115.6, 113.8, 79.1, 75.5, 66.9, 37.5, 28.4; HRMS (FAB): found 368.0587 [calcd for $C_{14}H_{15}ClN_5O_3S^+$ $(M + H)^+$ 368.0584]; Anal. Calcd for $C_{14}H_{14}ClN_5O_3S$: C, 45.72; H, 3.84; N, 19.04. Found: C, 45.75; H, 4.06; N, 19.39.

(2R,3R,4S)-2-(2-Chloro-8-(furan-2-yl)-6-((3-iodobenzyl)amino)-9H-purin-9-yl)tetrahydrothiophene-3,4-diol (5o).—Yield = 64%; white solid; mp 219 °C; $[\alpha]_D^{25} = -52.49$ (*c* 0.13, MeOH); UV (MeOH) λ_{max} 248, 311 nm; ^{1}H NMR (800 MHz, DMSO-d_6): δ 9.06 (t, *J* = 6.0 Hz, 1H), 8.03 (s, 1H), 7.75 (s, 1H), 7.60 (d, *J* = 7.7 Hz, 1H), 7.36 (d, *J* = 7.6 Hz, 1H), 7.12–7.14 (m, 2H), 6.79 (s, 1H), 6.17 (d, *J* = 7.8 Hz, 1H), 5.48 (d, *J* = 6.2 Hz, 1H), 5.35 (br s, 1H), 5.30 (br s, 1H), 4.57–4.63 (m, 2H), 4.38 (s, 1H), 3.46 (dd, *J* = 11.3, 3.4 Hz, 1H), 2.80 (d, *J* = 11.2 Hz, 1H); ^{13}C NMR (200 MHz, DMSO-d_6): δ 154.5, 152.5, 150.5, 145.6, 143.1, 142.1, 141.7, 136.0, 135.5, 130.5, 126.8, 118.9, 113.5, 112.2, 94.7, 76.2, 72.0, 64.1, 42.5, 35.6; HRMS (FAB): found 569.9866 [calcd for $C_{20}H_{18}ClIN_5O_3S^+$ $(M + H)^+$ 569.9864]; Anal. Calcd for $C_{20}H_{17}ClIN_5O_3S$: C, 42.16; H, 3.01; N, 12.29. Found: C, 42.55; H, 2.97; N, 12.61.

(2R,3R,4S)-2-(6-Amino-2-chloro-8-(thiophen-2-yl)-9H-purin-9-yl)tetrahydrothiophene-3,4-diol (5p).—Yield = 60%; white solid; mp 235 °C; $[\alpha]_D^{25} = -51.90$ (*c* 0.205, MeOH); UV (MeOH) λ_{max} 246, 303 nm; ^{1}H NMR (600 MHz, MeOD): δ 7.73 (dd, *J* = 5.0, 0.9 Hz, 1H), 7.71 (dd, *J* = 3.6, 0.9 Hz, 1H), 7.25 (dd, *J* = 4.9, 3.6 Hz, 1H), 6.20 (d, *J* = 7.3 Hz, 1H), 5.56 (dd, *J* = 7.8, 3.6 Hz, 1H), 4.52–4.53 (m, 1H), 3.67 (dd, *J* = 11.4, 3.1 Hz, 1H), 2.91 (dd, *J* = 11.4, 1.8 Hz, 1H); ^{13}C NMR (200 MHz, MeOD): δ 158.5, 155.3, 153.9, 148.7, 132.2, 131.77, 131.74, 130.0, 120.4, 78.8, 75.4, 66.9, 37.5; HRMS (FAB): found 370.0194 [calcd for $C_{13}H_{13}ClN_5O_2S_2^+$ $(M + H)^+$ 370.0199]; Anal. Calcd for $C_{13}H_{12}ClN_5O_2S_2$: C, 42.23; H, 3.29; N, 18.95. Found: C, 42.61; H, 3.01; N, 18.91.

(2R,3R,4S)-2-(2-Chloro-6-(methylamino)-8-(thiophen-2-yl)-9H-purin-9-yl)tetrahydrothiophene-3,4-diol (5q).—Yield = 58%; white solid; mp 236 °C; $[\alpha]_D^{25} = -81.42$ (*c* 0.10, MeOH);

UV (MeOH) λ_{max} 249, 311 nm; ^{1}H NMR (400 MHz, MeOD): δ 7.71 (dd, J = 5.0, 1.3 Hz, 1H), 7.68 (dd, J = 3.9, 0.9 Hz, 1H), 7.24 (dd, J = 5.0, 3.6 Hz, 1H), 6.19 (d, J = 7.3 Hz, 1H), 5.56 (dd, J = 7.3, 3.2 Hz, 1H), 4.52–4.53 (m, 1H), 3.67 (dd, J = 11.4, 3.6 Hz, 1H), 3.06 (br s, 3H), 2.90 (dd, J = 11.4, 1.8 Hz, 1H); ^{13}C NMR (200 MHz, MeOD): δ 160.3, 157.8, 155.8, 152.8, 148.1, 132.5, 131.5, 129.9, 121.0, 78.8, 75.4, 66.9, 37.4, 28.4; HRMS (FAB): found 384.0349 [calcd for $C_{14}H_{15}ClN_5O_2S_2^+$ $(M + H)^+$ 384.0356]; Anal. Calcd for $C_{14}H_{14}ClN_5O_2S_2$: C, 43.80; H, 3.68; N, 18.24. Found: C, 43.81; H, 3.60; N, 17.99.

(2R,3R,4S)-2-(2-Chloro-6-((3-iodobenzyl)amino)-8-(thiophen-2-yl)-9H-purin-9-yl)tetrahydrothiophene-3,4-diol (5r).—Yield = 55%; white solid; mp 207 °C; $[\alpha]_D^{25} = -77.58$ (c 0.12, MeOH); UV (MeOH) λ_{max} 252, 310 nm; ^{1}H NMR (600 MHz, MeOD): δ 7.79 (br s, 1H), 7.71 (d, J = 5.0 Hz, 1H), 7.69 (d, J = 3.6 Hz, 1H), 7.60 (d, J = 7.8 Hz, 1H), 7.40 (d, J = 7.8 Hz, 1H), 7.24 (dd, J = 5.0, 3.7 Hz, 1H), 7.09 (t, J = 7.8 Hz, 1H), 6.20 (d, J = 7.8 Hz, 1H), 5.57 (dd, J = 7.8, 3.6 Hz, 1H), 4.66–4.74 (m, 2H), 4.51–4.53 (m, 1H), 3.67 (dd, J = 11.4, 3.6 Hz, 1H), 2.90 (dd, J = 11.4, 1.8 Hz, 1H); ^{13}C NMR (200 MHz, DMSO-d_6): δ 154.4, 152.3, 150.9, 145.6, 141.8, 136.1, 135.5, 130.5, 130.4, 130.2, 129.2, 128.2, 126.8, 118.8, 94.7, 75.9, 71.8, 64.1, 42.5, 35.6; HRMS (FAB): found 585.9620 [calcd for $C_{20}H_{18}ClIN_5O_2S_2^+$ $(M + H)^+$ 585.9635]; Anal. Calcd for $C_{20}H_{17}ClIN_5O_2S_2$: C, 41.00; H, 2.92; N, 11.95. Found: C, 41.40; H, 2.50; N, 11.55.

General Procedure for N^2-Amination for the Synthesis of 5s-5v.—To a solution of **5m**, **5n**, **5p**, and **5q** in anhydrous 1-butanol (0.10 M) was dropwise added *N,N*-diisopropylethylaminetriethylamine (10.00 equiv) followed by tyramine (5.00 equiv) at room temperature. After being heated with microwave at 180 °C for 2 h, the reaction mixture was cooled to room temperature and evaporated. The residue was purified by silica gel column chromatography (CH_2Cl_2/MeOH, 25/1) to give **5s–5v**.

(2R,3R,4S)-2-(6-Amino-8-(furan-2-yl)-2-((4-hydroxyphenethyl)-amino)-9H-purin-9-yl)tetrahydrothiophene-3,4-diol (5s).—Yield = 63%; yellow solid; mp 232 °C; $[\alpha]_D^{25} = 16.16$ (c 0.10, MeOH); UV (MeOH) λ_{max} 228, 324 nm; ^{1}H NMR (800 MHz, MeOD): δ 7.75 (d, J = 1.2 Hz, 1H), 7.05 (d, J = 8.4 Hz, 2H), 7.04 (d, J = 3.2 Hz, 1H), 6.69–6.71 (m, 2H), 6.66 (dd, J = 3.4, 1.8 Hz, 1H), 6.27 (d, J = 7.2 Hz, 1H), 5.72–5.75 (m, 1H), 4.53 (dd, J = 5.6, 3.3 Hz, 1H), 3.59 (dd, J = 11.5, 3.6 Hz, 1H), 3.56 (t, J = 7.2 Hz, 2H), 2.87 (dd, J = 11.5, 2.2 Hz, 1H), 2.83 (t, J = 7.2 Hz, 2H); ^{13}C NMR (200 MHz, DMSO-d_6): δ 158.7, 156.0, 155.4, 154.8, 144.3, 144.2, 138.0, 132.1, 130.3, 130.0, 129.3, 115.0, 114.9, 111.7, 111.3, 79.1, 78.9, 75.7, 72.6, 35.7, 34.5; HRMS (FAB): found 455.1439 [calcd for $C_{21}H_{23}N_6O_4S^+$ $(M + H)^+$ 455.1435]; Anal. Calcd for $C_{21}H_{22}N_6O_4S$: C, 55.49; H, 4.88; N, 18.49. Found: C, 55.51; H, 4.85; N, 18.51.

(2R,3R,4S)-2-(8-(Furan-2-yl)-2-((4-hydroxyphenethyl)amino)-6-(methylamino)-9H-purin-9-yl)tetrahydrothiophene-3,4-diol (5t).—Yield = 65%; pale yellow solid; mp 262 °C; $[\alpha]_D^{25} = -3.12$ (c 8.67, MeOH); UV (MeOH) λ_{max} 219, 287, 327 nm; ^{1}H NMR (800 MHz, MeOD): δ 7.72 (d, J = 1.2 Hz, 1H), 7.05 (d, J = 8.4 Hz, 2H), 6.99 (d, J = 3.1 Hz, 1H), 6.70–6.71 (m, 2H), 6.63 (dd, J = 3.4, 1.8 Hz, 1H), 6.26 (d, J = 7.2 Hz, 1H), 5.73 (br s, 1H), 4.53 (dd, J = 3.2, 5.6 Hz, 1H), 3.60 (dd, J = 11.4, 3.5 Hz, 1 H),

3.58 (s, 1H), 3.57 (s, 1H), 3.02 (br s, 3H), 2.87 (dd, J = 11.5, 2.1 Hz, 1H), 2.83 (t, J = 7.4 Hz, 2H); ^{13}C NMR (200 MHz, DMSO-d_6): δ 158.7, 155.4, 155.3, 155.2, 151.4, 144.4, 144.2, 137.6, 130.0, 129.3, 115.0, 114.3, 111.7, 111.1, 75.8, 72.6, 63.9, 62.7, 43.1, 35.7, 34.6, 26.8; HRMS (FAB): found 469.1670 [calcd for $C_{22}H_{25}N_6O_4S^+$ $(M + H)^+$ 469.1658]; Anal. Calcd for $C_{22}H_{24}N_6O^4S$: C, 56.40; H, 5.16; N, 17.94. Found: C, 56.12; H, 5.00; N, 17.86.

(2R,3R,4S)-2-(6-Amino-2-((4-hydroxyphenethyl)amino)-8-(thiophen-2-yl)-9H-purin-9-yl)tetrahydrothiophene-3,4-diol (5u).—Yield = 66%; pale yellow solid; mp 165 °C; $[\alpha]_D^{25} = -91.28$ (c 0.185, MeOH); UV (MeOH) λ_{max} 231, 324 nm; ^{1}H NMR (800 MHz, DMSO-d_6): δ 9.15 (s, 1H), 7.74 (dd, J = 5.0, 0.9 Hz, 1H), 7.48 (dd, J = 3.4, 0.7 Hz, 1H), 7.24 (dd, J = 5.1, 3.6 Hz, 1H), 7.02 (d, J = 7.9 Hz, 2H), 6.79 (br s, 2H), 6.68–6.69 (m, 2H), 6.39 (t, J = 5.7 Hz, 1H), 5.98 (d, J = 7.6 Hz, 1H), 5.62 (br s, 1H), 5.46 (br s, 1H), 5.26 (br s, 1H), 4.36 (s, 1H), 3.44 (d, J = 10.9 Hz, 1H), 3.41 (dd, J = 14.8, 5.4 Hz, 2H), 2.78 (dd, J = 11.2, 1.7 Hz, 1H), 2.73–2.75 (m, 2H); ^{13}C NMR (200 MHz, DMSO-d_6): δ 158.6, 155.9, 155.4, 152.7, 141.1, 132.0, 130.1, 129.38, 129.35, 128.3, 127.9, 127.6, 115.08, 115.05, 113.8, 72.5, 63.9, 62.7, 43.1, 35.7, 34.6; HRMS (FAB): found 471.1268 [calcd for $C_{21}H_{23}N_6O_3S_2^+$ $(M + H)^+$ 471.1273]; Anal. Calcd for $C_{21}H_{22}N_6O_3S_2$: C, 53.60; H, 4.71; N, 17.86. Found: C, 53.41; H, 4.68; N, 17.94.

(2R,3R,4S)-2-(2-((4-Hydroxyphenethyl)amino)-6-(methylamino)-8-(thiophen-2-yl)-9H-purin-9-yl)tetrahydrothiophene-3,4-diol (5v).—Yield = 60%; pale yellow solid; mp 195 °C; $[\alpha]_D^{25} = -0.93$ (c 3.38, MeOH); UV (MeOH) λ_{max} 219, 331 nm; ^{1}H NMR (800 MHz, DMSO-d_6): δ 9.15 (s, 1H), 7.73 (dd, J = 5.1, 0.9 Hz, 1H), 7.47 (d, J = 2.9 Hz, 1H), 7.33 (br s, 1H), 7.24 (dd, J = 5.1, 3.6 Hz, 1H), 7.02 (d, J = 8.2 Hz, 2H), 6.68 (d, J = 8.4 Hz, 2H), 6.54 (br s, 1H), 5.98 (d, J = 7.6 Hz, 1H), 5.62 (br s, 1H), 5.44 (br s, 1H), 5.25 (s, 1H), 4.36 (s, 1H), 3.41–3.45 (m, 3H), 2.89 (br s, 2H), 2.75–2.79 (m, 3H); ^{13}C NMR (200 MHz, DMSO-d_6): δ 158.6, 155.4, 155.0, 151.9, 140.7, 132.1, 130.1, 130.1, 129.3, 128.2, 127.9, 127.4, 115.0, 115.0, 114.1, 75.6, 72.5, 63.9, 43.1, 35.7, 34.6, 26.8; HRMS (FAB): found 485.1432 [calcd for $C_{22}H_{25}N_6O_3S_2^+$ $(M + H)^+$ 485.1430]; Anal. Calcd for $C_{22}H_{24}N_6O_3S_2$: C, 54.53; H, 4.99; N, 17.34. Found: C, 54.31; H, 4.67; N, 17.36.

Molecular Docking Study.

The crystal structures of A_{2A}AR containing the A_{2A}AR agonist (NECA) or antagonists (LJ-4517, ZM-241385) were used for the molecular docking study. (PDB ID: 2YDV, 3EML, 8CU6). The preparation of ligands and proteins and homology modeling of A_3AR with the crystal structure of A_{2A}AR (PDB ID: 8CU6) were performed by Maestro 13.0 (Schrödinger, LLC, New York, NY, 2021). The grid generation and ligand docking were progressed in a Glide docking program in Maestro 13.0, and the predicted binding mode was calculated as XP-precision.

Pharmacological Assays.

Cell Culture and Membrane Preparation.—HEK293 cells expressing recombinant hA_1AR, hA_{2A}AR, or A_3AR were cultured in Dulbecco's modified Eagle's medium supplemented with 10% fetal bovine serum, 100 units/mL penicillin, 100 μg/mL streptomycin, and 2 μmol/mL glutamine. Cells were collected by scraping into ice-cold

PBS buffer. After homogenization and suspension, cells were centrifuged at 1000*g* or 10 min, and the pellet was discarded. The suspension was then recentrifuged at 20,000*g* for 60 min at 4 °C. The resultant pellets were resuspended in buffer containing 3 units/mL adenosine deaminase (from bovine spleen, Worthington Biochemical Corp., Lakewood, NJ) and incubated at 37 °C for 30 min. The aliquots of membrane preparation were kept at −80 °C until further use.

Binding Assays at hA_1AR and $hA_{2A}AR$.—For binding to hA_1AR, 50 μL of increasing concentrations of a test ligand and 50 μL of **25** (1.0 nM, PerkinElmer, Boston, MA) were incubated with membrane preparations (40 μg/tube) at 25 °C for 60 min in 50 mM Tris·HCl buffer (pH 7.4) containing 10 mM $MgCl_2$ in a total assay volume of 200 μL. Nonspecific binding was determined using 10 μM of **29**. For $hA_{2A}AR$ binding, membrane preparations (20 μg/tube) were incubated at 25 °C for 60 min with a final concentration of **26** (5 nM, American Radiolabeled Chemicals, Inc., St. Louis, MO) in a mixture containing 50 μL of increasing concentrations of a test ligand and 200 μL of 50 mM Tris·HCl, pH 7.4, containing 10 mM $MgCl_2$. **29** (10 μM) was used to define nonspecific binding. The reaction was terminated by filtration with GF/B filters. Filters were placed in scintillation vials containing 5 mL of Hydrofluor scintillation liquid and counted using a PerkinElmer Tricarb 2810TR liquid scintillation counter.

Binding Assays at $hA_{2B}AR$.—Adenosin A_{2B} receptor competition binding experiments were carried out in a multiscreen GF/C 96-well plate. In each well was incubated 25 μg of membranes from the Euroscreen HEK-A2B cell line and prepared in our laboratory (lot: A009/14–02–2020, protein concentration = 5254.8 μg/mL), 25 nM of **27** (140 Ci/mmol, 1 mCi/mL, PerkinElmer NET974001MC) and compounds studied and standard. Nonspecific binding was determined in the presence of 1000 μM of **29** (Sigma E2397). The reaction mixture (Vt: 250 μL/well) was incubated at 25 °C for 30 min, 200 μL was transferred to GF/C 96-well plate (Millipore, Madrid, Spain) pretreated with binding buffer (Tris-HCl 50 mM, EDTA 1 mM, $MgCl_2$ 5 mM, bacitracin 100 μg/μL, adenosine deaminase 2 U/mL, pH = 6.5), which was then filtered and washed 4 times with 250 μL wash buffer (Tris-HCl 50 mM, EDTA 1 mM, $MgCl_2$ 5 mM, pH = 6.5) before measuring in a microplate β scintillation counter (MicroBeta Trilux, PerkinElmer, Madrid, Spain).

Binding Assay at hA_3AR.—Each tube in the binding assay contained 100 μL of membrane suspension (10 μg protein), 50 μL of **28** (0.2 nM, PerkinElmer, Boston, MA), and 50 μL of increasing concentrations of the test ligands in Tris·HCl buffer (50 mM, pH 8.0) containing 10 mM $MgCl_2$. Nonspecific binding was determined using 10 μM of **29**. The mixtures were incubated at 25 °C for 60 min. Binding reaction was terminated by filtration through Whatman GF/B filters using a MT-24 cell harvester (Brandel, Gaithersburg, MD, USA). Filters were washed 3 times with 9 mL of ice-cold buffer. Filters were counted using a PerkinElmer Cobra II γ-counter.

Cyclic AMP Accumulation Assay.—Human adenosine receptor functional experiments were carried out in the CHO-A_{2A} cell line and the CHO-A_3 cell line for $hA_{2A}AR$ and hA_3AR, respectively. The day before the assay, the cells are seeded on the 96 well culture

plate (Falcon 353072). The cells are washed with wash buffer [Dulbecco's modified Eagle's medium nutrient mixture F-12 ham (Sigma D8062), 25 mM Hepes; pH = 7.4]. Wash buffer is replaced by incubation buffer [Dulbecco's modified Eagle's medium nutrient mixture F-12 ham (Sigma D8062), 25 mM Hepes, 30 μM rolipram (Sigma R6520); pH = 7.4]. Test compounds are added and incubated at 37 °C for 15 min. Afterward, 1 μM of **29** (Sigma E2387) is added and incubated at 37 °C for 15 min. Also, for hA_3AR, FSK (Sigma F3917) is added and incubated at 37 °C for 5 min. After incubation, the amount of cAMP is determined using the cAMP Biotrak Enzymeimmunoassay (EIA) System Kit (GE Healthcare RPN225).

Statistical Analysis.—Binding and functional parameters were calculated using Prism 5.0 software (GraphPAD, San Diego, CA, USA). IC_{50} values obtained from competition curves were converted to K_i values using the Cheng–Prusoff equation.[32] Data were expressed as mean ± standard error of the mean.

Pharmacokinetic Assay.—For pharmacokinetic studies, CrljOr-i:CD1 male mice were obtained as weanlings of 6 weeks of age upon arrival (provided by DBL Co., Ltd.). This study was reviewed and approved by the Institutional Animal Care and Use Committees (IACUC) of Chaon Co., Ltd. (IACUC number: CE21077). Mice weighed about 31.4 g; animals were 7 weeks old at the start of dosing. For the single pharmacokinetics (i.v.: 2 mg/5 mL/kg; oral: 10 mg/10 mL/kg) of compound **5d** in mice, the dosing solution was 5% DMSO/40% PEG 400/55% DW (v/v/v). This study was conducted using a cross-over ($n = 3$) design. Blood samples (0.1 mL) were collected from the retro-orbital plexus at 5, 15, and 30 min and 1, 2, 4, 8, 12, and 24 h postdose for the i.v. group and 15, 30 min, and 1, 2, 4, 8, 12, and 24 h postdose for the oral group. The collected blood samples were placed in heparinized tubes (5 IU/mL). Plasma was obtained by centrifugation at 5000 rpm for 5 min at 4 °C. Aliquots of plasma (30–40 μL) were transferred to polypropylene tubes and stored at −15 °C until analysis. LC–MS/MS was used to determine the concentration of the compound **5d** at plasma. To measure the concentration of compound **5d** at plasma, selectivity, linearity, and stability in plasma (at 10 °C for 4 h) were confirmed. *In vivo* PK data were analyzed using Phoenix WinNonlin software (Phoenix WinNonlin 8.3). A noncompartment model analysis was performed to obtain the following parameters: AUC_{0-t}, C_0 or C_{max}, T_{max}, clearance (CL), volume of distribution (V_{ss}), half-life ($t_{1/2}$), and bioavailability (F).

In Vivo Tumor Xenograft Model.—All animal experiments were conducted according to the guidelines approved by the Seoul National University Institutional Animal Care and Use Committee (IACUC; permission number: SNU-190408–5). Female mice (BALB/c, aged 4–5 weeks, weighing 18 g) were purchased from the Central Laboratory Animal, Inc. (Seoul, Korea), and they were housed under pathogen-free conditions with a 12 h light–dark schedule. 4T1-Luc cells were then injected subcutaneously into the flanks of mice (1×10^6 cells in 200 μL of 50:50 PBS/Matrigel), and tumors were allowed to grow for 7 days until their volume reached approximately 50 mm^3. The mice were randomized into vehicle control and treatment groups ($n = 5$). Vehicle control (DMSO/cremophor/normal saline = 5:5:90), **5d** (10 mg/kg body weight), antimouse PD-L1 (10 mg/kg body weight), or a

combination of **5d** (10 mg/kg body weight) and antimouse PD-L1 (10 mg/kg body weight) was administered intraperitoneally (i.p.) 3 times per week for 21 days; mice were then euthanized 1 week later. Tumors were excised, weighed, and frozen for further biochemical analysis. Tumor volume was measured using an electronic caliper according to the following formula: tumor volume (mm^3) = 3.14 × length × width × height/6. Toxicity was evaluated based on body weight loss. Bioluminescence images of mice were acquired on the final day of the experiment. Mice were anesthetized, positioned in the IVIS (PerkinElmer, Waltham, MA, USA), and imaged 15 min after injection of D-luciferin (150 mg/kg, Gold Biotechnology) resuspended in PBS.

Supplementary Material

Refer to Web version on PubMed Central for supplementary material.

ACKNOWLEDGMENTS

This work was supported by the Basic Science Research Program through the National Research Foundation of Korea (NRF) funded by the Ministry of Education (NRF-2022R1A6A1A0304624712), the Mid-Career Researcher Programs (NRF-2021R1A2B5B0200154413 and 2021M3E5E308084321) of the National Research Foundation of Korea (NRF), Korea, and in part by the Intramural Research Program of the NIH, National Institute of Diabetes and Digestive and Kidney Diseases (ZIADK031117).

ABBREVIATIONS

AUC	area under the curve
AR	adenosine receptor
cAMP	cyclic adenosine-5′-monophosphate
BSA	bis(trimethylsilyl)-acetamide
CGS21680	2-[*p*-(2-carboxyethyl)-phenylethylamino]-5′-*N*-ethylcarboxamidoadenosine
CHO	Chinese hamster ovary
CKD	chronic kidney disease
Cl-IB-MECA	2-chloro-N^6-(3-iodobenzyl)-5′-*N*-methylcarbamoyladenosine
CYP	cytochrome P450
DIBAL-H	diisobutylaluminum hydride
HEK	human embryonic kidney
hERG	human ether-a-go-go related gene
I-AB-MECA	N^6-(4-amino-3-iodobenzyl)-5′-*N*-methylcarboxamidoadenosine

IVIS	*in vivo* imaging system
LDA	lithium diisopropylamide
LiTMP	lithium tetramethylpiperidide
mAb	monoclonal antibody
NECA	5′-*N*-ethylcarboxamidoadenosine
PBS	phosphate buffered saline
PD-L1	programmed death-ligand 1
PKC	protein kinase C
PLC	phospholipase C
PPTS	pyridinium *p*-toluenesulfonate
***p*TSA**	*para*-toluene sulfonic acid
***R*-PIA**	(−)-N^6-2-phenylisopropyl adenosine
SAR	structure—activity relationship
TBAF	tetra-*n*-butylammonium fluoride
TBS	*t*-butyldimethylsilyl
thio-Cl-IB-MECA	2-chloro-N^6-(3-iodobenzyl)-5′-N-methylcarbamoyl–4′-thioadenosine
TMSOTf	trimethylsilyl trifluoromethanesulfonate
Tris-HCl	tris(hydroxymethyl)aminomethane hydrochloride

REFERENCES

(1). Sung H; Ferlay J; Siegel RL; Laversanne M; Soerjomataram I; Jemal A; Bray F Global Cancer Statistics 2020: GLOBOCAN Estimates of Incidence and Mortality Worldwide for 36 Cancers in 185 Countries. Ca-Cancer J. Clin 2021, 71, 209–249. [PubMed: 33538338]

(2). (a) Waldman AD; Fritz JM; Lenardo MJ A guide to cancer immunotherapy: from T cell basic science to clinical practice. Nat. Rev. Immunol 2020, 20, 651–668. [PubMed: 32433532] (b) Darvin P; Toor SM; Sasidharan Nair V; Elkord E Immune checkpoint inhibitors: recent progress and potential biomarkers. Exp. Mol. Med 2018, 50 (12), 1–11.(c) Marin-Acevedo JA; Kimbrough EO; Lou Y Next generation of immune checkpoint inhibitors and beyond. J. Hematol. Oncol 2021, 14, 45. [PubMed: 33741032]

(3). (a) Robert C. A decade of immune-checkpoint inhibitors in cancer therapy. Nat. Commun 2020, 11, 3801. [PubMed: 32732879] (b) Johnson DB; Nebhan CA; Moslehi JJ; Balko JM Immune-checkpoint inhibitors: long-term implications of toxicity. Nat. Rev. Clin. Oncol 2022, 19, 254–267. [PubMed: 35082367]

(4). Liu C; Seeram NP; Ma H Small molecule inhibitors against PD-1/PD-L1 immune checkpoints and current methodologies for their development: a review. Cancer Cell Int. 2021, 21, 239. [PubMed: 33906641]

(5). Dhanak D; Edwards JP; Nguyen A; Tummino PJ Small-Molecule Targets in Immuno-Oncology. Cell Chem. Biol 2017, 24, 1148–1160. [PubMed: 28938090]

(6). Ohta A. A Metabolic Immune Checkpoint: Adenosine in Tumor Microenvironment. Front. Immunol 2016, 7, 109. [PubMed: 27066002]

(7). Haskó G; Linden J; Cronstein B; Pacher P Adenosine receptors: therapeutic aspects for inflammatory and immune diseases. Nat. Rev. Drug Discovery 2008, 7 (9), 759–770. [PubMed: 18758473]

(8). Sevigny CP; Li L; Awad AS; Huang L; McDuffie M; Linden J; Lobo PI; Okusa MD Activation of adenosine 2A receptors attenuates allograft rejection and alloantigen recognition. J. Immunol 2007, 178 (7), 4240–4249. [PubMed: 17371980]

(9). (a) Leone RD; Lo YC; Powell JD A2aR antagonists: Next generation checkpoint blockade for cancer immunotherapy. Comput. Struct. Biotechnol. J 2015, 13, 265–272. [PubMed: 25941561] (b) Mediavilla-Varela M; Castro J; Chiappori A; Noyes D; Hernandez DC; Allard B; Stagg J; Antonia SJ A Novel Antagonist of the Immune Checkpoint Protein Adenosine A2a Receptor Restore Tumor Infiltrating Lymphocyte Activity in the Context of the Tumor Microenvironment. Neoplasia 2017, 19 (7), 530–536. [PubMed: 28582704]

(10). Yu F; Zhu C; Xie Q; Wang Y Adenosine A2A Receptor Antagonists for Cancer Immunotherapy. J. Med. Chem 2020, 63 (21), 12196–12212. [PubMed: 32667814]

(11). Shiriaeva A; Park D; Kim G; Lee Y; Hou X; Jarhad DB; Kim G; Yu J; Hyun YE; Kim W; Gao ZG; Jacobson KA; Han GW; Stevens RC; Jeong LS; Choi S; Cherezov V GPCR Agonist-to-Antagonist Conversion: Enabling the Design of Nucleoside Functional Switches for the A_{2A} Adenosine Receptor. J. Med. Chem 2022, 65 (17), 11648–11657. [PubMed: 35977382]

(12). Lee HW; Son SH; Kang JY; Jang HJ; Ahn SY; Kim JW; Byun JS; Ji SH; Kim SH; Choi JR Adenosine derivative having antagonistic action on A2a and A3 adenosine receptors and method for preparing same. WO 2022203427 A1, September 29, 2022.

(13). Kim HO; Ji X.-d.; Siddiqi SM; Olah ME; Stiles GL; Jacobson KA 2-Substitution of N^6-benzyladenosine-5′-uronamides enhances selectivity for A_3-adenosine receptors. J. Med. Chem 1994, 37, 3614–3621. [PubMed: 7932588]

(14). (a) Jeong LS; Jin DZ; Kim HO; Shin DH; Moon HR; Gunaga P; Chun MW; Kim Y-C; Melman N; Gao Z-G; Jacobson KA N^6-Substituted D-4′-thioadenosine-5′-methyluronamides: potent and selective agonists at the human A_3 adenosine receptor. J. Med. Chem 2003, 46, 3775–3777. [PubMed: 12930138] (b) Jeong LS; Lee HW; Jacobson KA; Kim HO; Shin DH; Lee JA; Gao Z-G; Lu C; Duong HT; Gunaga P; Lee SK; Jin DZ; Chun MW; Moon HR Structure-activity relationships of 2-chloro-N^6-substituted-4′-thioadenosine-5′-methyluronamides as highly potent and selective agonists at the human A_3 adenosine receptor. J. Med. Chem 2006, 49, 273–281. [PubMed: 16392812] (c) Choi WJ; Lee HW; Kim HO; Chinn M; Gao Z-G; Patel A; Jacobson KA; Moon HR; Jung YH; Jeong LS Design and synthesis of N^6-substituted-4′-thioadenosine-5′-uronamides as potent and selective human A_3 adenosine receptor agonists. Bioorg. Med. Chem 2009, 17, 8003–8011. [PubMed: 19879151]

(15). (a) Jeong LS; Choe SA; Gunaga P; Kim HO; Lee HW; Lee SK; Tosh DK; Patel A; Palaniappan KK; Gao Z-G; Jacobson KA; Moon HR Discovery of a new nucleoside template for human A_3 adenosine receptor ligands: D-4′-thioadenosine derivatives without 4′-hydroxymethyl group as highly potent and selective antagonists. J. Med. Chem 2007, 50, 3159–3162. [PubMed: 17555308] (b) Jeong LS; Pal S; Choe SA; Choi WJ; Jacobson KA; Gao Z-G; Klutz AM; Hou X; Kim HO; Lee HW; Lee SK; Tosh DK; et al. Structure-activity relationships of truncated D- and L-4′-thioadenosine derivatives as species- independent A_3 adenosine receptor antagonists. J. Med. Chem 2008, 51, 6609–6613. [PubMed: 18811138] (c) Pal S; Choi WJ; Choe SA; Heller CL; Gao Z-G; Chinn M; Jacobson KA; Hou X; Lee SK; Kim HO; Jeong LS Structure-activity relationships of truncated adenosine derivatives as highly potent and selective human A_3 adenosine receptor antagonists. Bioorg. Med. Chem 2009, 17, 3733–3738. [PubMed: 19375920] (d) Choi WJ; Park JG; Yoo SJ; Kim HO; Moon HR; Chun MW; Jung YH; Jeong LS Syntheses of D- and L-Cyclopentenone derivatives using ring-closing metathesis: Versatile intermediates for the synthesis of D- and L-carbocyclic nucleosides. J. Org. Chem 2001, 66, 6490–6494. [PubMed: 11559205]

(16). Lee J; Hwang I; Lee JH; Lee HW; Jeong LS; Ha H The selective A3AR antagonist LJ-1888 ameliorates UUO-induced tubulointerstitial fibrosis. Am. J. Pathol 2013, 183, 1488–1497. [PubMed: 24001475]

(17). Kim H; Kang JW; Lee S; Choi WJ; Jeong LS; Yang Y; Hong JT; Yoon DY A_3 Adenosine receptor antagonist, truncated Thio-Cl-IB-MECA, induces apoptosis in T24 human bladder cancer cells. Anticancer Res. 2010, 30, 2823–2830. [PubMed: 20683018]

(18). (a) Hou X; Kim HO; Alexander V; Kim K; Choi S; Park S; Lee JH; Yoo LS; Gao Z; Jacobson KA; Jeong LS Discovery of a new human A_{2A} adenosine receptor agonist, truncated 2-hexynyl-4′-thioadenosine. ACS Med. Chem. Lett 2010, 1, 516–520.(b) Hou X; Majik MS; Kim K; Pyee Y; Lee Y; Alexander V; Chung HJ; Lee HW; Chandra G; Lee JH; Park S.-g.; Choi WJ; Kim HO; Phan K; Gao Z-G; Jacobson KA; Choi S; Lee SK; Jeong LS Structure—activity relationships of truncated C2- or C8-substituted adenosine derivatives as dual acting A_{2A} and A_3 adenosine receptor ligands. J. Med. Chem 2012, 55, 342–356. [PubMed: 22142423]

(19). Ballesteros JA; Weinstein H [19] Integrated methods for the construction of three-dimensional models and computational probing of structure-function relations in G protein-coupled receptors. Methods Neurosci. 1995, 25, 366–428.

(20). (a) Xu F; Wu H; Katritch V; Han GW; Jacobson KA; Gao Z-G; Cherezov V; Stevens RC Structure of an agonist-bound human A_{2A} adenosine receptor. Science 2011, 332, 322–327. [PubMed: 21393508] (b) Lebon G; Warne T; Edwards PC; Bennett K; Langmead CJ; Leslie AGW; Tate CG Agonist-bound adenosine A_{2A} receptor structure reveal common features of GPCR activation. Nature 2011, 474, 521–525. [PubMed: 21593763] (c) Carpenter B; Lebon G Human Adenosine A_{2A} Receptor: Molecular Mechanism of Ligand Binding and Activation. Front. Pharmacol 2017, 8, 898. [PubMed: 29311917]

(21). Vorbrüggen H; Ruh-Pohlenz C Synthesis of nucleosides. Org. React 2004, 55, 1–630.

(22). Ibrahim N; Chevot F; Legraverend M Regioselective Sonogashira cross-coupling reactions of 6-chloro-2,8-diiodo-9-THP-9H-purine with alkyne derivatives. Tetrahedron Lett. 2011, 52, 305–307.

(23). Kim G; Lee G; Kim G; Seo Y; Jarhad DB; Jeong LS Catalyst-controlled Regioselctive Sonogashira Coupling of 9-Sub-stituted-6-chloro-2,8-diiodopurines. Org. Chem. Front 2022, 9, 5536–5543.

(24). (a) Sonogashira K Development of Pd-Cu catalyzed cross-coupling of terminal acetylenes with sp^2-carbon halides. J. Organomet. Chem 2002, 653, 46–49.(b) Chinchilla R; Najera C The Sonogashira reaction: a booming methodology in synthetic organic chemistry. Chem. Rev 2007, 107, 874–922. [PubMed: 17305399]

(25). Stille JK The palladium-catalyzed cross-coupling reactions of organotin reagents with organic electrophiles. Angew. Chem., Int. Ed. Engl 1986, 25, 508–524.

(26). Qu S; Mulamoottil VA; Nayak A; Ryu S; Hou X; Song J; Yu J; Sahu PK; Zhao LX; Choi S; Lee SK; Jeong LS Design, synthesis, and anticancer activity of C8-substituted-4′-thionucleosides as potential HSP90 inhibitors. Bioorg. Med. Chem 2016, 24, 3418–3428. [PubMed: 27283788]

(27). (a) Robins RK; Godefroi EF; Taylor EC; Lewis LR; Jackson A Purine nucleosides. I. The synthesis of certain 6-substituted-9-(tetrahydro-2-pyranyl)-purines as models of purine deoxynucleosides. J. Am. Chem. Soc 1961, 83, 2574–2579.(b) Cassidy F; Olsen RK; Robins RK Aromaticity in heterocyclic system V. Bromination of certain purines, pyrrolo[3,2-*d*]pyrimidines and pyrazolo[4,3-*d*]pyrimidines (1). J. Heterocycl. Chem 1968, 5, 461–465.

(28). Ongini E; Dionisotti S; Gessi S; Irenius E; Fredholm BB Comparison of CGS 15943, ZM 241385 and SCH 58261 as antagonist at human adenosine receptors. Naunyn-Schmiedeberg's Arch. Pharmacol 1999, 359, 7–10. [PubMed: 9933143]

(29). Nayak A; Chandra G; Hwang I; Kim K; Hou X; Kim HO; Sahu PK; Roy KK; Yoo J; Lee Y; Cui M; Choi S; Moss SM; Phan K; Gao Z-G; Ha H; Jacobson KA; Jeong LS Synthesis and anti-renal fibrosis activity of conformationally locked truncated 2-hexynyl-N^6-substituted-(*N*)-methano carbanucleosides as A_3 adenosine receptor antagonists and partial agonists. J. Med. Chem 2014, 57, 1344–1354. [PubMed: 24456490]

(30). (a) Beno BR; Yeung KS; Bartberger MD; Pennington LD; Meanwell NA A Survey of the Role of Noncovalent Sulfur Interactions in Drug Design. J. Med. Chem 2015, 58, 4383–4438. [PubMed: 25734370] (b) It also could be observed in the crystal structures of **11b, 22a**, and **22b**.

(31). (a) Merighi S; Benini A; Mirandola P; Gessi S; Varani K; Leung E; MacLennan S; Baraldi PG; Borea PA A^3 Adenosine Receptors Modulate Hypoxia-Inducible Factor-1A Expression in Human A375 Melanoma Cells. Neoplasia 2005, 7, 894–903. [PubMed: 16242072] (b) Flamant L; Notte N; Ninane N; Raes M; Michiels C Anti-apoptotic role of HIF-1 and AP-1 in paclitaxel exposed breast cancer cells under hypoxia. Mol. Cancer 2010, 9, 191. [PubMed: 20626868] (c) Merighi S; Benini A; Mirandola P; Gessi S; Varani K; Leung E; Maclennan S; Borea PA A_3 Adenosine Receptor Activation Inhibits Cell Proliferation via Phosphatidylinositol 3-Kinase/Akt-dependent Inhibition of the Extracellular Signal-regulated Kinase 1/2 Phosphorylation in A375 Human Melanoma Cells. J. Biol. Chem 2005, 280 (20), 19516–19526. [PubMed: 15774470] (d) Brambilla R; Cattabeni F; Ceruti S; Barbieri D; Franceschi C; Kim YC; Jacobson K; Klotz KN; Lohse M; Abbracchio M Activation of the A3 adenosine receptor affects cell cycle progression and cell growth. Naunyn-Schmiedeberg's Arch. Pharmacol 2000, 361, 225–234. [PubMed: 10731034]

(32). Yung-Chi C; Prusoff WH Relationship between the inhibition constant (K_i and the concentration of inhibitor which causes 50% inhibition (IC_{50}) of an enzymatic reaction. Biochem. Pharmacol 1973, 22, 3099–3108. [PubMed: 4202581]

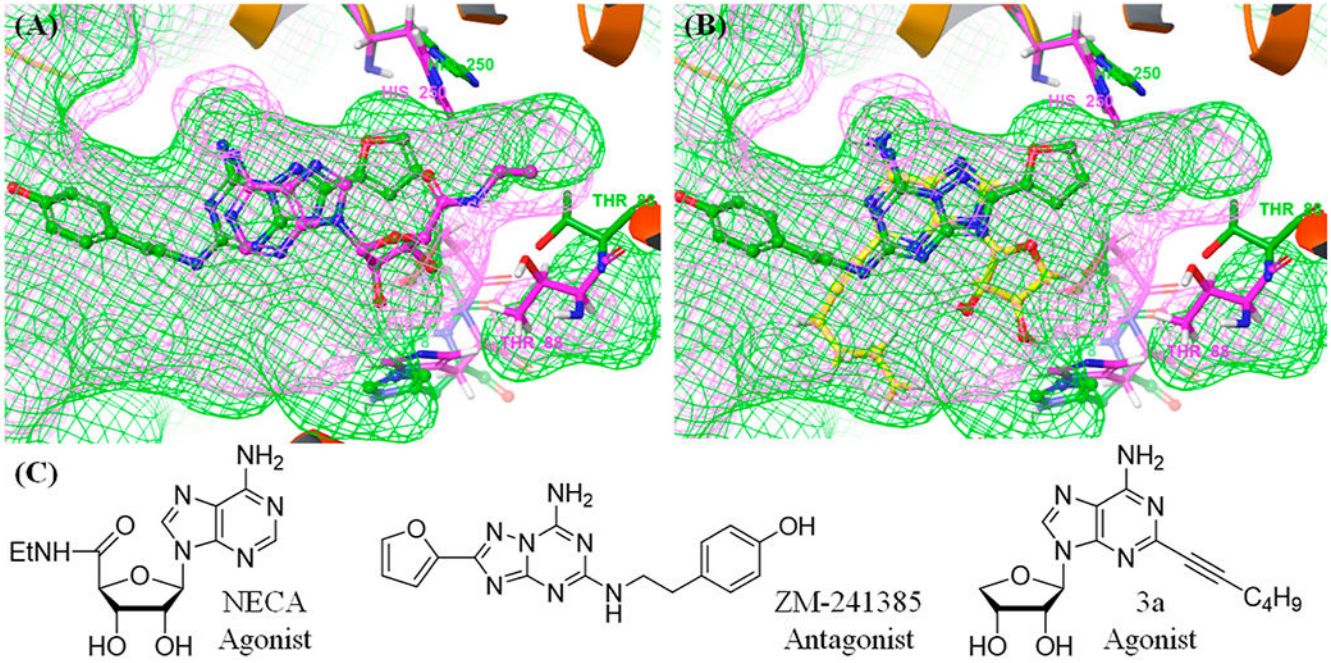

Figure 1.

X-ray co-crystal structure of $hA^{2A}AR$ containing NECA (pink, PDB ID: 2YDV) and ZM-241385 (green, PDB ID: 3EML). (A) Comparison of the binding pocket for the co-crystal structures and its subpocket. (B) Predicted binding mode of **3a** with $hA_{2A}AR$ (yellow, PDB ID: 3EML). (C) Chemical structures of the ligands.

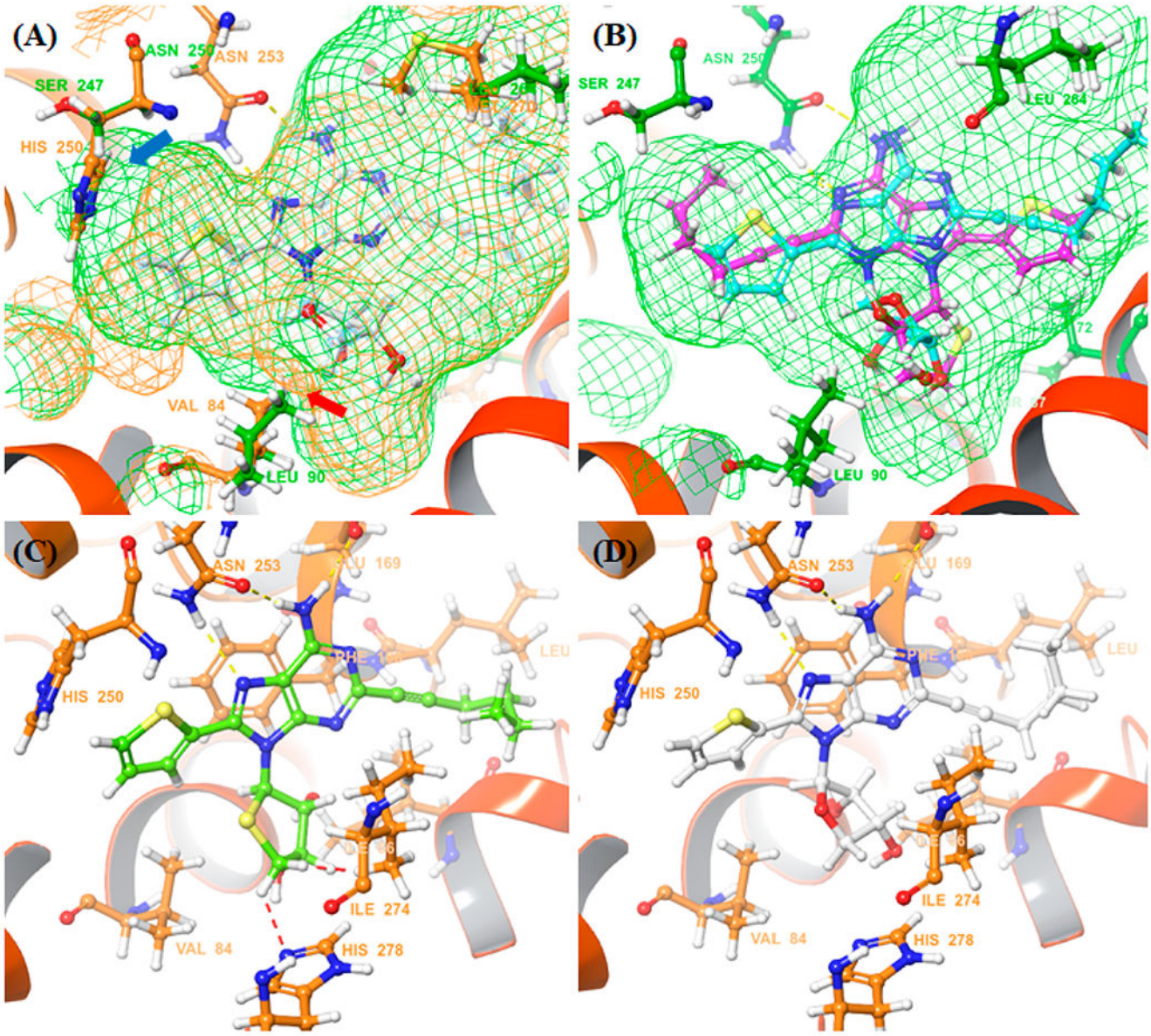

Figure 2.

Comparison of the crystal structure of $hA_{2A}AR$ (PDB ID: 8CU6) and the homology model of A_3AR. (A) Binding pocket of the co-crystal structure of $hA_{2A}AR$ (orange), and the homology model of A_3AR. (green) (B) Predicted binding mode of **5d** (cyan) and **5j** (magenta) for hA_3AR. (C) Predicted binding mode of **5j** (lime) and (D) co-crystal structure of **5d** (white) with $hA_{2A}AR$. The red dashed line represents steric clashes, and the yellow dashed line represents hydrogen bonding.

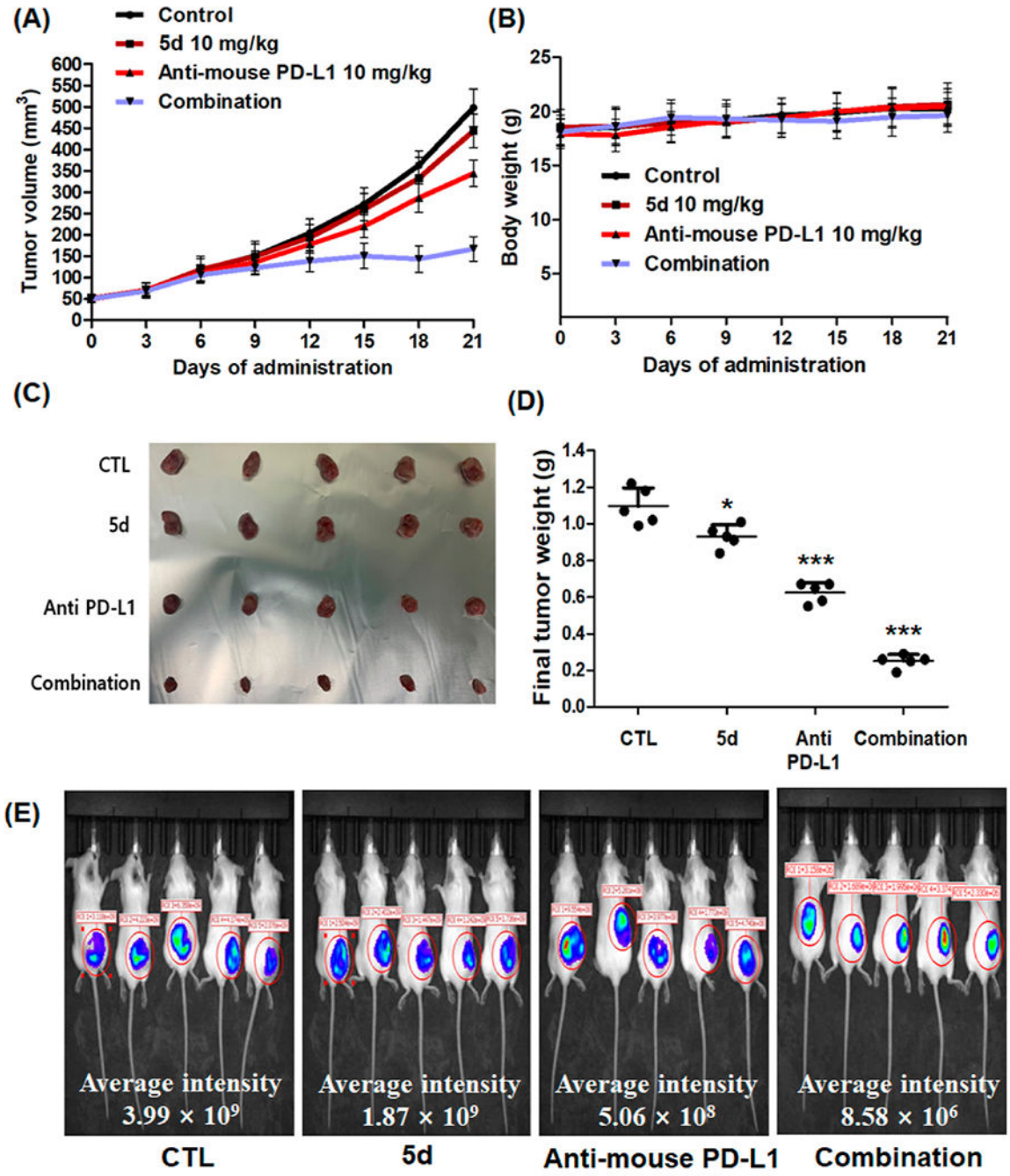

Figure 3.

In vivo antitumor activity of the compound **5d** and its synergistic effect with immune checkpoint inhibitor. Mice bearing 4T1-Luc tumors were treated thrice per week with vehicle (DMSO/cremophor/normal saline = 5:5:90), **5d** (10 mg/kg, i.p.), anti-PD-L1 (10 mg/kg, i.p.), or combination of **5d** (10 mg/kg, i.p.), and anti-PD-L1 (10 mg/kg, i.p.). (A) Tumor volume and (B) body weight of the mice bearing 4T1-Luc tumors during administration. (C) Image of excised tumors from the mice and (D) their tumor weight. (E) Luciferase imaging (IVIS) of the mice on the final day of the experiment. Average signal

intensity was measured by PerkinElmer Living Image software. *$P < 0.05$, **$P < 0.01$, ***$P < 0.001$ *vs* the control.

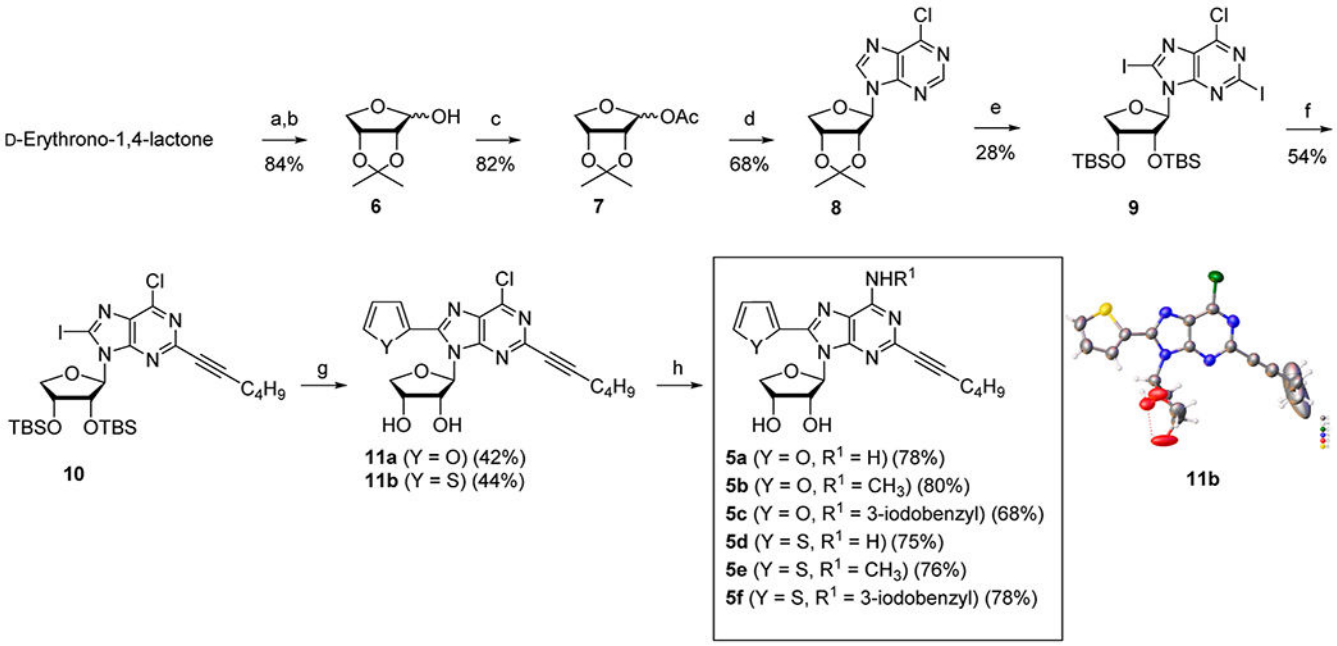

Scheme 1. Synthesis of Truncated 2-Hexynyl-*N*^{6},8-Disubstituted-Adenosines 5a–f[a]

[a]Reagents and conditions: (a) *p*TSA, 2,2-dimethoxypropane, DMF, 4 h, reflux; (b) DIBAL-H, toluene, −78 °C, 30 min; (c) AC_2O, pyridine, rt, 3 h; (d) 6-chloropurine, HMDS, $(NH_4)_2SO_4$, TMSOTf, 1,2-dichloroethane, 0 to 80 °C, 15 h; (e) (i) 1 N HCl, THF, rt, 15 h; (ii) TBSCl, imidazole, DMF, rt, 15 h; (iii) tetramethylpiperidine, I_2, *n*-BuLi, THF, −78 °C, 4 h; (f) $Pd(PPh_3)_4$, Cs_2CO_3, CuI, 1-hexyne, DMF, rt, 5 h; (g) (i) $Pd(PPh_3)_2Cl_2$, 2-tributylstannylfuran, THF, 70 °C, 1 h for **11a** or $Pd(PPh_3)_2Cl_2$, 2-tributylstannylthiophene, THF, 60 °C, 1 h for **11b**; (ii) Et_3N, $Et_3N{\cdot}3HF$, THF, rt, 15 h; (h) NH_3/*t*-BuOH, 100 °C, 12 h for **5a**, **5d** and $CH_3NH_2{\cdot}HCl$, Et_3N, EtOH, rt, 24 h for **5b**, **5e**, and 3-iodobenzylamine·HCl, Et_3N, EtOH, rt, 24 h for **5c** and **5f**.

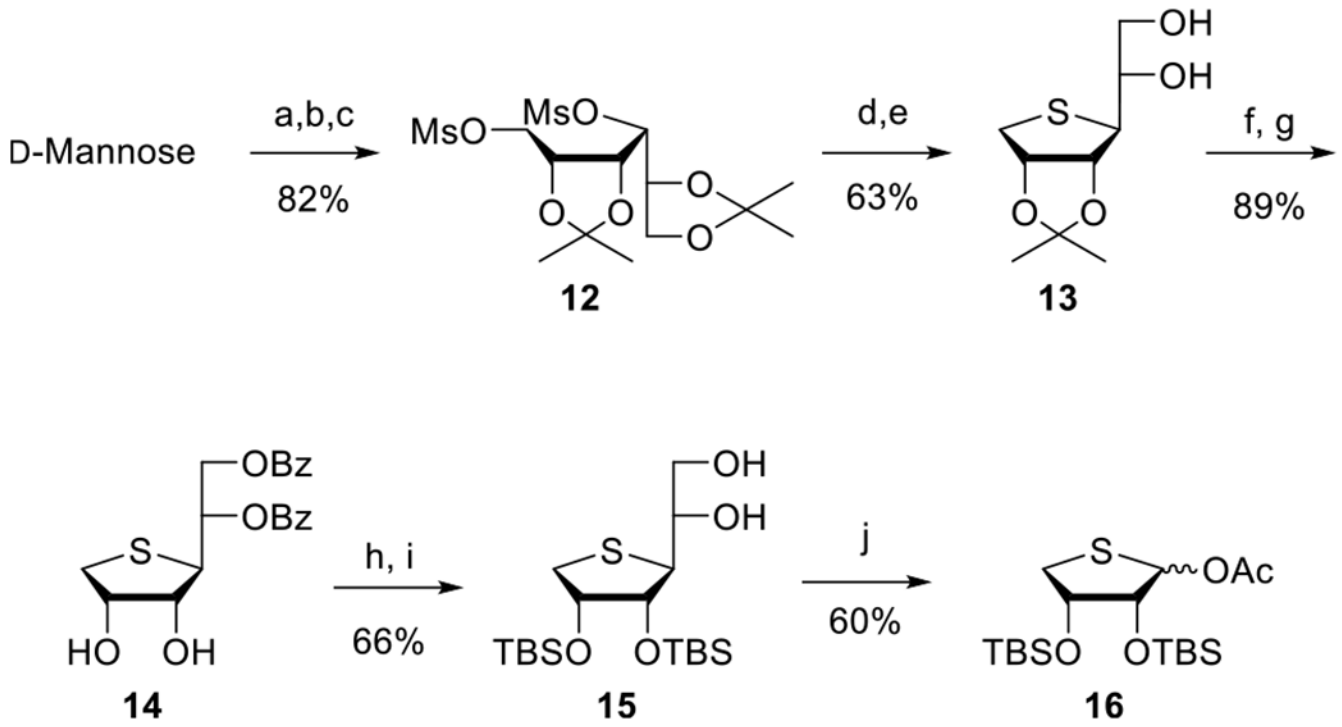

Scheme 2. Synthesis of the Glycosyl Donor 16[a]

[a]Reagents and conditions: (a) 2,2-dimethoxypropane, camphorsulfonic acid, acetone, rt, 15 h; (b) $NaBH_4$, EtOH, rt, 2 h; (c) MsCl, Et_3N, CH_2Cl_2, rt, 1 h; (d) Na_2S, DMF, 80 °C, 15 h; (e) 60% AcOH, rt, 2 h; (f) BzCl, pyridine, CH_2Cl_2, rt, 18 h; (g) 80% AcOH, 70 °C, 12 h; (h) TBSCl, imidazole, DMF, rt, 18 h; (i) NaOMe, MeOH, rt, 2 h; (j) $Pb(OAc)_4$, EtOAc, rt, 18 h.

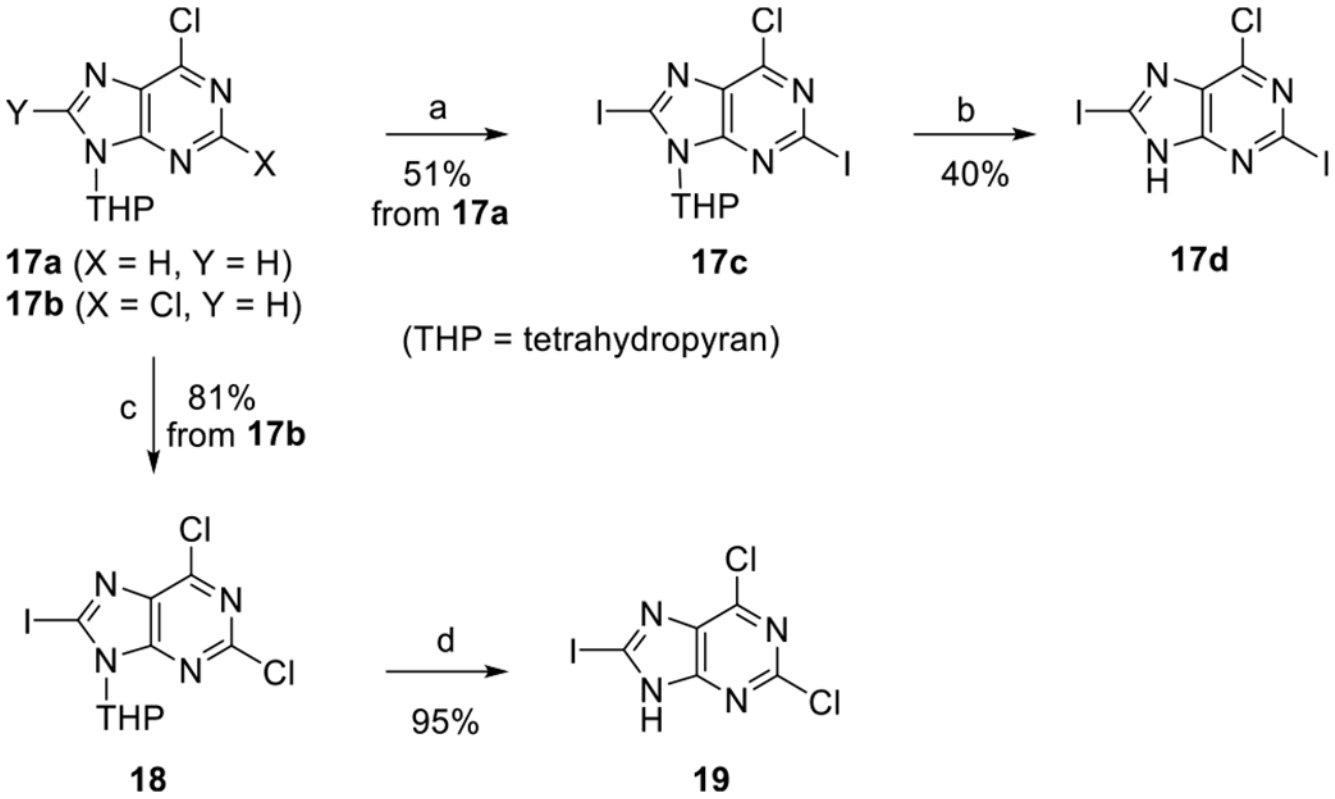

Scheme 3. Synthesis of 6-Chloro-2,8-diiodopurine 17d and 2,6-Dichloro-8-iodopurine 19[a]

[a]Reagents and conditions: (a) tetramethylpiperidine, I_2, *n*-BuLi, THF, −78 °C, 4 h; (b) $CuCl_2$, EtOH/H_2O, 85 °C, 5 h; (c) *i*-Pr_2NH, *n*-BuLi, I_2, THF, −78 °C, 2 h; (d) PPTS, EtOH, 60 °C, 6 h.

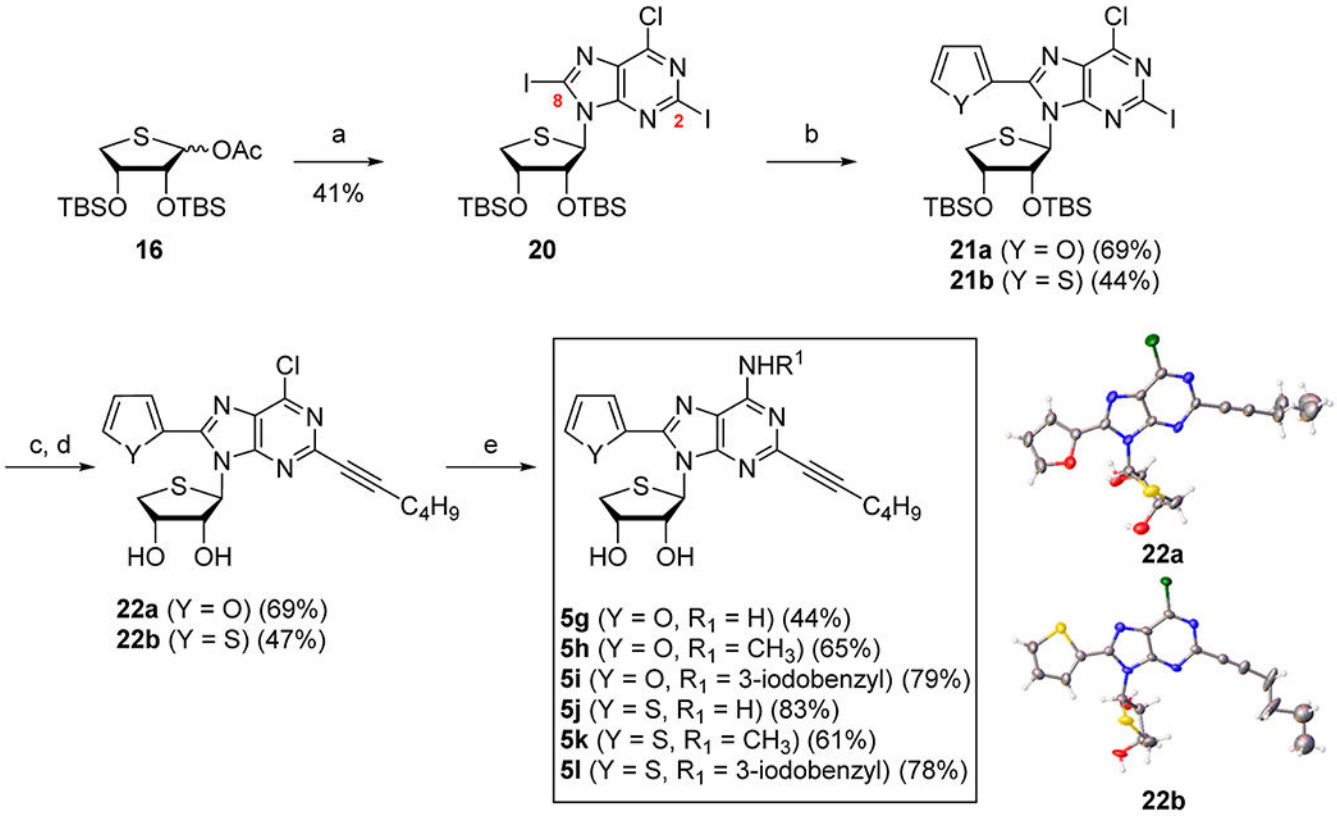

Scheme 4. Synthesis of Truncated 2-Hexynyl-*N*^{6},C8-Disubstituted-4′-Thioadenosines 5g–l[a]

[a]Reagents and conditions: (a) **17d**, BSA, TMSOTf, CH_3CN, 75 °C, 1.5 h; (b) $Pd(dba)_2$, 2-tributylstannylfuran, DMF/PhMe, rt, 9 h for **21a** or $Pd(dba)_2$, 2-tributylstannylthiophene, DMF/PhMe, rt, 23 h for **21b**; (c) $Pd(PPh_3)_2Cl_2$, 1-hexyne, CuI, Cs_2CO_3, DMF, rt, 14 h for **22a** or 16 h for **22b**; (d) *n*-Bu_4NF, THF, rt, 16 h for **22a** or 50 °C, 12 h for **22b**; (e) NH_3/*t*-BuOH, 100 °C, 15 h for **5g**, **5j** or CH_3NH_2·HCl, Et_3N, EtOH, 50 °C, 23 h for **5h** or 28 h for **5k** or 3-iodobenzylamine·HCl, Et_3N, EtOH, 50 °C, 24 h for **5i** or 75 °C, 20 h for **5l**.

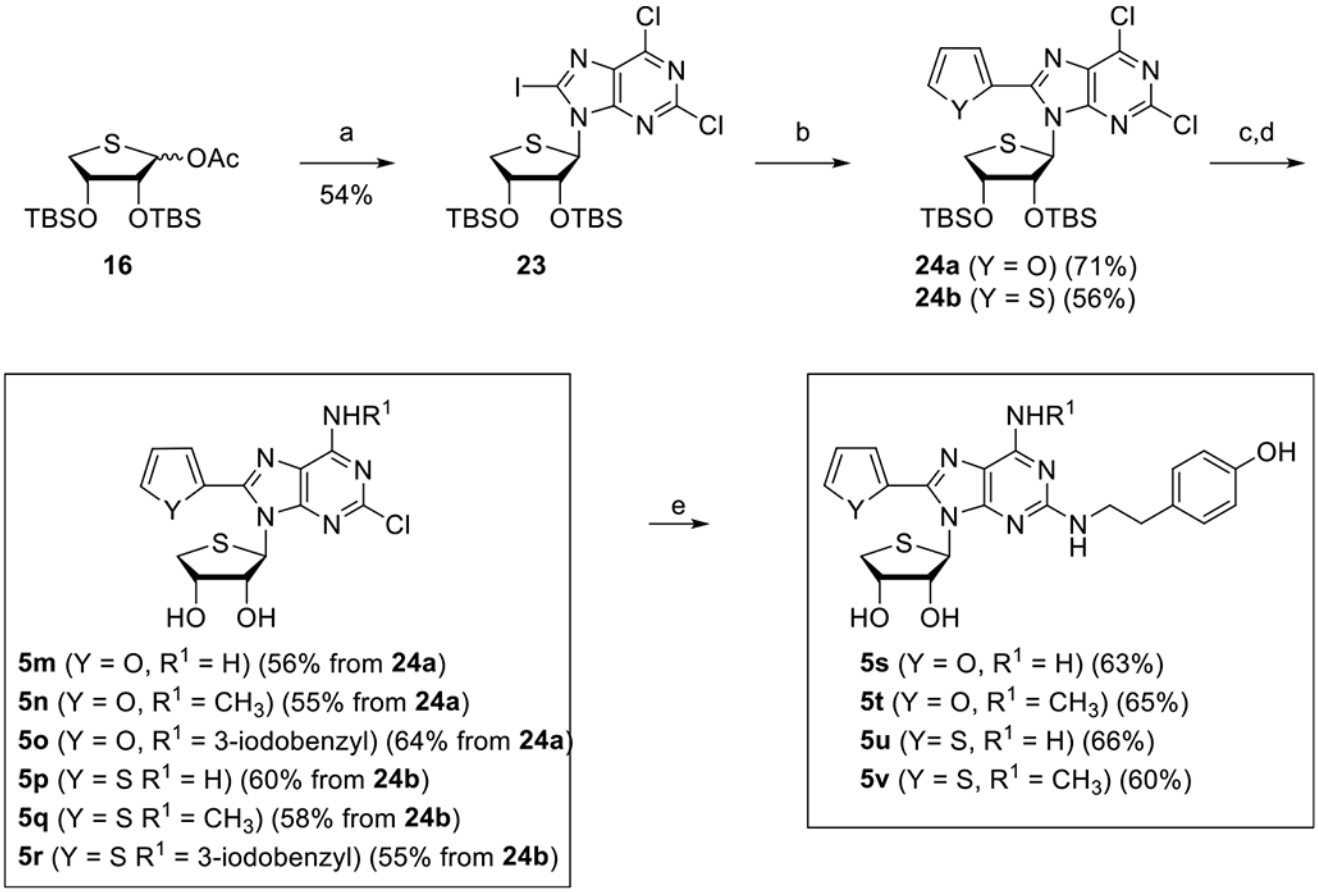

Scheme 5. Synthesis of Truncated 2-Chloro- and 2-*p*-Hydroxyphenethylamino-*N*^{6},C8-Disubstituted-4′-Thioadenosines 5m–v[a]

[a]Reagents and conditions: (a) **19**, BSA, TMSOTf, CH_3CN, 75 °C, 1.5 h; (b) $Pd(PPh_3)_2Cl_2$, 2-tributylstannylfuran, THF, 70 °C, 24 h for **24a** or $Pd(PPh_3)_2Cl_2$, 2-tributylstannylthiophene, THF, 70 °C, 24 h for **24b**; (c) TBAF, THF, rt, 1 h; (d) NH_3/*t*-BuOH, 120 °C, 15 h for **5m**, **5p** or CH_3NH_2·HCl, Et_3N, EtOH, rt, 24 h for **5n**, **5q** or 3-iodobenzylamine·HCl, Et_3N, EtOH, rt, 24 h for **5o**, **5r**; (e) tyramine, DIPEA, 1-butanol, MW, 180 °C, 2 h.

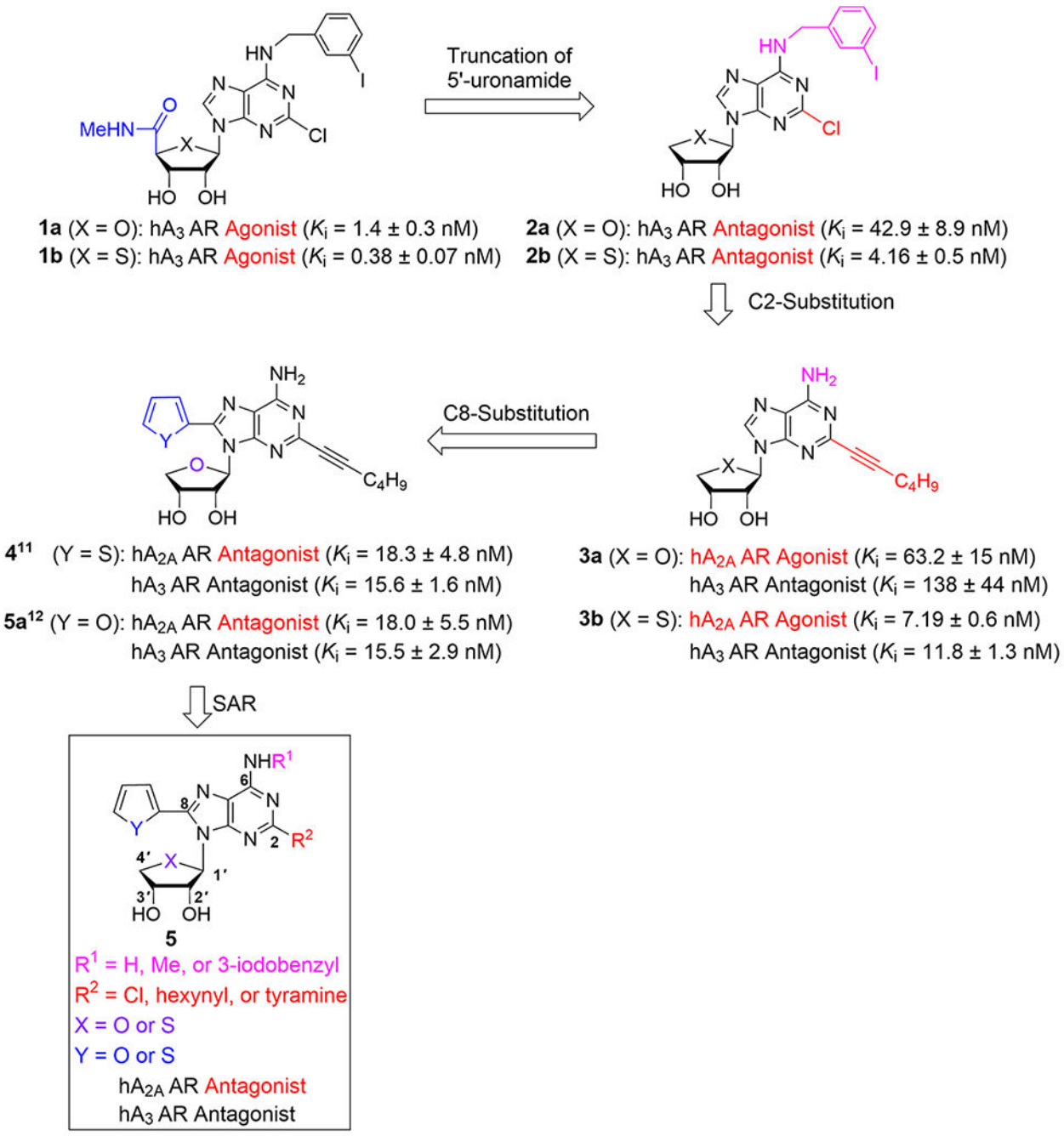

Chart 1.
Rationale for the Design of the Target Nucleosides 5

J Med Chem. Author manuscript; available in PMC 2024 September 14.

Table 1.

Binding Affinities of Compounds 5a–v at Four Subtypes of the hARs

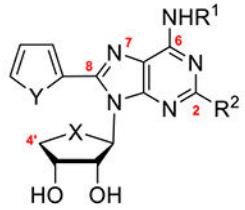

5a-v

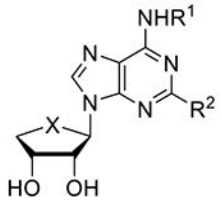

3a, b

compd no.	X	Y	R^1	R^2	K_i value (nM ± SEM[a] or % displacement at 10 μM[b])			
					hA_1AR	$hA_{2A}AR$	$hA_{2B}AR$	hA_3AR
5a	O	O	H	1-hexyne	183 ± 28	18.0 ± 5.5	327 ± 32	15.5 ± 2.9
5b	O	O	CH_3	1-hexyne	3030 ± 50	50.5 ± 12.1	76 ± 1%	2.9 ± 0.7
5c	O	O	3-I-Bn	1-hexyne	13 ± 1%	579 ± 53	4 ± 2%	199 ± 20
5d = 4	O	S	H	1-hexyne	392 ± 99	7.7 ± 0.5	834 ± 11	15.6 ± 1.6
5e	O	S	CH_3	1-hexyne	2310 ± 600	126 ± 18	52 ± 1%	2.9 ± 0.5
5f	O	S	3-I-Bn	1-hexyne	2580 ± 460	513 ± 153	2 ± 3%	8.9 ± 4.8
5g	S	O	H	1-hexyne	46 ± 1%	13.2 ± 0.2	1973 ± 251	119 ± 39
5h	S	O	CH_3	1-hexyne	17 ± 9%	159 ± 17	41 ± 2%	53.5 ± 16.9
5i	S	O	3-I-Bn	1-hexyne	11 ± 7%	5 ± 5%	3 ± 2%	2 ± 8%
5j	S	S	H	1-hexyne	494 ± 122	61.4 ± 4.1	27 ± 2%	150 ± 6
5k	S	S	CH_3	1-hexyne	11 ± 3%	2820 ± 1080	11 ± 2%	206 ± 26
5l	S	S	3-I-Bn	1-hexyne	1 ± 0.2%	2 ± 2%	3 ± 3%	12 ± 5%
5m	S	O	H	Cl	3890 ± 650	140 ± 10	53 ± 3%	855 ± 157
5n	S	O	CH_3	Cl	49 ± 1%	752 ± 67	46 ± 1%	94.6 ± 45.2
5o	S	O	3-I-Bn	Cl	4900 ± 1070	336 ± 108	51 ± 1%	89.7 ± 20.4
5p	S	S	H	Cl	1980 ± 140	459 ± 46	62 ± 3%	294 ± 80
5q	S	S	CH_3	Cl	26 ± 4%	955 ± 704	17 ± 1%	138 ± 10
5r	S	S	3-I-Bn	Cl	50 ± 2%	720 ± 9	17 ± 2%	137 ± 28

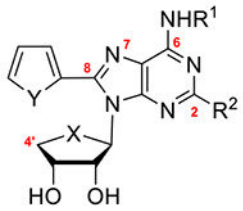

5a-v

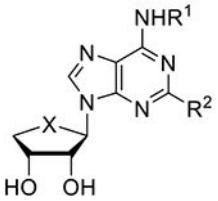

3a, b

compd no.	X	Y	R^1	R^2	K_i value (nM ± SEM[a] or % displacement at 10 μM[b])			
					hA_1AR	$hA_{2A}AR$	$hA_{2B}AR$	hA_3AR
5s	S	O	H	tyramine	46 ± 3%	112 ± 6	227 ± 41	1650 ± 100
5t	S	O	CH_3	tyramine	5330 ± 340	468 ± 28	713 ± 88	445 ± 148
5u	S	S	H	tyramine	8050 ± 910	946 ± 94	608 ± 81	3010 ± 1140
5v	S	S	CH_3	tyramine	47 ± 2%	917 ± 59	579 ± 135	106 ± 27
3a[c]	S		H	1-hexyne	39 ± 10%	7.19 ± 0.6	N.D.[d]	11.8 ± 1.3
3b[c]	O		H	1-hexyne	740 ± 430	63.2 ± 15	N.D.[d]	138 ± 44

[a] All binding experiments were performed using adherent CHO cells and HEK293 cells stably transfected with cDNA encoding the appropriate hAR binding was carried out using 1 nM **25**, 10 nM **26**, 25 nM **27**, and 0.2 nM **28** as radioligands for A_1, A_{2A}, A_{2B}, and A_3ARs, respectively. Values are expressed as mean ± SEM, n ± 3–4 (outliers eliminated), and are normalized against a nonspecific binder, **29**.

[b] When a percent value is shown, it refers to the percent inhibition of a specific radioligand binding at 10 μM, with nonspecific binding defined using 10 μM of 29.

[c] Ref 18.

[d] Not determined.

Table 2.

cAMP Functional Assay Data at $hA_{2A}AR$ and hA^3AR Expressed in CHO Cells[a]

compound no.	% activation, A_{2A} cAMP assay	% activation, A_3 cAMP assay
5a	0.3 ± 0.3	16 ± 4
5d	0.8 ± 0.3	4 ± 4
5g	0.05 ± 0.1	11 ± 5

[a]At a concentration of 10 μM, unless noted.

Table 3.

In Vivo Pharmacokinetic Properties of Compound 5d

PK parameter	route of dosing	
	i.v. (*n* = 3)	p.o. (*n* = 3)
dose (mg/kg)	2.00	10.00
AUC_{0-t} (h·ng/mL)	550.95	626.55
C_{max} (ng/mL)	1984.94	1241.79
T_{max} (h)	0.08	0.25
CL ((mL/min)/kg)	60.5	
V_{ss} (L/kg)	0.69	
$t_{1/2}$ (h)	0.16	1.99
F (%)		22.81